

## Chapter 5: Photochemistry and Surface Chemistry

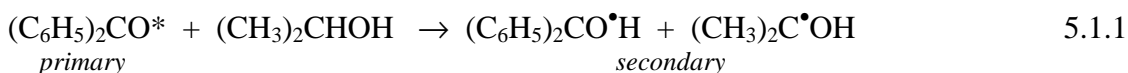
Calculate the steady-state concentration of ozone in the stratosphere.

The theory of chemical kinetics provides the techniques necessary to model chemical reactions under a wide variety of circumstances. Chemical kinetics is a powerful tool to explore the interrelationships among diverse processes. For example, processes in atmospheric and aquatic environments couple photochemical and surface reactions to homogeneous processes in the gas and aqueous phase. In the next two chapters we apply our basic theoretical understanding to applications in photochemistry, surface chemistry, and systems that couple chemical reactions with concentration gradients. An understanding of these areas is required to make progress in unraveling important issues in biogeochemical chemistry, biochemistry, medicine, and energy technology. The primary example in our discussion of photochemistry will be the photochemical mechanism that determines the ozone balance in the stratosphere. Our examples for surface chemistry will include biochemical interaction analysis and surface catalysis.

### 5.1 Photochemistry

Sunlight is the source of energy for most all chemical processes. A few counter examples include sulfur-reducing bacteria near deep-sea thermal vents or thermochemical processes driven by nuclear reactors and geothermal energy. Sunlight is the direct source of energy for photosynthesis. We are currently highly dependent on photosynthetic processes that occurred roughly 30-350 million years ago through the use of coal, oil, and natural gas. The development of new biofuels and solar based biomass conversion processes is an attempt to make more direct and efficient use of the light from the sun for production of transportation fuels, home heating, and industrial feed stocks. Photochemical processes are also important in laboratory synthesis, biogeochemical cycles, and industrial production. How do we express the rates of photochemical processes?

The two general laws for photochemistry are that light must be absorbed by a molecule to initiate a photochemical process, and each absorbed photon results in one primary photochemical process. This second law is called the **Stark-Einstein Law of photochemical equivalence**. **Primary** photochemical processes are the direct result of the absorption of light. **Secondary** photochemical processes do not necessarily require the absorption of light. Primary photochemical processes include direct bond dissociation, ionization, and the formation of reactive molecular excited states. An example of direct bond dissociation from the  $H_2 + Br_2$  reaction is the free radical chain initiation from the photolysis of  $Br_2$  in Eq. 4.3.3. After the photochemical initiation, the subsequent reactions in the free radical chain mechanism are secondary processes. An example of the formation of a reactive molecular excited state is the absorption of UV light by benzophenone. In isopropanol solution, the excited state of benzophenone then rapidly reacts with isopropanol to produce benzophenone ketyl  $(C_6H_5)_2CO^{\bullet}H$  and the isopropanol free radical, which are secondary photochemical products (see Problem 3.8):



The “\*” indicates an electronic excited state. The key result from the Stark-Einstein law is that one and only one photon is required to produce the primary photochemical intermediate. For

example, the energy required to break the bond in Br<sub>2</sub> is 190.2 kJ mol<sup>-1</sup>. One absorbed photon must supply at least this amount of energy, which from  $E = hc/\lambda$  corresponds to a maximum wavelength of (see Section 2.4):

$$\lambda = \frac{hc}{E/N_A} = \frac{6.626 \times 10^{-34} \text{ J s } (2.998 \times 10^8 \text{ m s}^{-1})}{(190.2 \times 10^3 \text{ J mol}^{-1} / 6.022 \times 10^{23} \text{ mol}^{-1})} = 628.9 \text{ nm} \quad 5.1.2$$

with  $N_A$  as Avogadro's number. Light redder than this value will not break the Br-Br bond, even with an increase in intensity. The Stark-Einstein Law holds for conventional light sources, including the sun. However, intense lasers can produce multi-photon processes that violate the Stark-Einstein one-photon-one-excited state rule. There is intense interest in studies of multi-photon excitation; however for this chapter we will consider only processes that follow the Stark-Einstein Law.

Photochemical processes require the absorption of light. Consider a reaction vessel with path length  $\ell$  with a light source of incident flux  $J_o$  and transmitted flux  $J$ , Figure 2.4.1. The flux absorbed by the solution is  $J_a = J_o - J$ , which from Eqs. 2.4.3 and 2.5.6 is given by:

$$J_a = J_o(1 - e^{-2.303 \epsilon[A]}) \quad (\text{J m}^{-2} \text{ s}^{-1}) \quad 5.1.3$$

where  $[A]$  is the concentration of the molecule that absorbs the light and  $\epsilon$  is the molar absorption coefficient of the solution. The absorbed flux is the rate of production of primary photoproducts. After the light is absorbed, many processes can occur. The excited molecule may lose energy by fluorescence, phosphorescence, chemical reactions such as Eq. 5.1.1, and non-radiative processes. The yield of fluorescence, phosphorescence, or any photochemical product may be determined by a **quantum yield**. For example, if the fluorescence light flux for the irradiated sample is  $J_f$  and the flux of absorbed light is  $J_a$ , then the fluorescence quantum yield is:

$$\Phi_f = J_f/J_a \quad 5.1.4$$

The quantum yield is a strong function of wavelength and can be defined for a narrow range of wavelengths or for a broad range of wavelengths.

The yield of any photochemical product can also be expressed as a quantum yield. We need to be careful with units, however. The quantum yield is unitless. The units of flux are  $\text{J m}^{-2} \text{ s}^{-1}$ , or equivalently  $\text{W m}^{-2}$ . Chemical concentrations are in units of moles per unit volume. For example, the molar flux of incident photons, with energy  $E = h\nu$ , in units of  $\text{mol m}^{-2} \text{ s}^{-1}$  is:

$$J_o' = \frac{J_o}{N_A h\nu} \quad (\text{mol m}^{-2} \text{ s}^{-1}) \quad 5.1.5$$

The energy of one mole of photons is called an Einstein, so the units of  $J_o'$  can also be listed as einsteins  $\text{m}^{-2} \text{ s}^{-1}$ . If the incident beam has a cross sectional area,  $\mathcal{A}$ , the moles of incident photons per second is  $J_o'\mathcal{A}$  for the irradiated volume  $V$ . The moles of photons per unit volume of the solution, in  $\text{mol L}^{-1} \text{ s}^{-1}$  is:<sup>1</sup>

$$J_o = J_o' \left( \frac{\mathcal{A}}{V} \right) = \frac{J_o}{N_A h\nu} \left( \frac{\mathcal{A}}{V} \right) \quad (\text{mol L}^{-1} \text{ s}^{-1}) \quad 5.1.6$$

with  $\mathcal{A}$  in  $\text{m}^2$  and  $V$  in  $\text{L}$ , with the flux in  $\text{J m}^{-2} \text{ s}^{-1}$ . Unfortunately, the symbols for the flux,  $J_o$ ,  $J_o'$ ,  $\Phi_o$ , and  $I_o$ , are all used interchangeably in the literature, the only difference being the units. You need to determine the units from the context. The absorbed flux in  $\text{mol L}^{-1} \text{ s}^{-1}$  is, from Eq. 5.1.3:

$$J_a = J_o (1 - e^{-2.303 \epsilon l[A]}) = \frac{J_o}{N_A h\nu} \left( \frac{A}{V} \right) (1 - e^{-2.303 \epsilon l[A]}) \quad (\text{mol L}^{-1} \text{ s}^{-1}) \quad 5.1.7$$

The rate law for the production of primary photoproduct,  $[A^*]$  is then equal to the absorbed flux:

$$\frac{d[A^*]}{dt} = J_a = J_o (1 - e^{-2.303 \epsilon l[A]}) \quad (\text{mol L}^{-1} \text{ s}^{-1}) \quad 5.1.8$$

with the rate in  $\text{mol L}^{-1} \text{ s}^{-1}$ . This last equation has two useful specific limits. If the reaction vessel is very thick or if the molar absorbance is very large then the exponential term approaches zero,  $e^{-2.303 \epsilon l[A]} \rightarrow 0$ , and all incident light is absorbed giving:

$$\frac{d[A^*]}{dt} = J_a = J_o = \frac{J_o}{N_A h\nu} \left( \frac{A}{V} \right) \quad (\epsilon l[A] \gg 1) \quad 5.1.9$$

which is zeroth order in A. This limit is useful, for example, for concentrated solutions or also for processes within the euphotic zone in a lake, where by definition all the light is absorbed (at least to 99%). The other limit is a solution or gas that has a small absorbance, so the exponential factor can be expanded in a Taylor series,  $e^{-2.303 \epsilon l[A]} \approx 1 - 2.303 \epsilon l[A]$ , and then the absorbed flux using Eq. 5.1.7 simplifies to:

$$J_a = 2.303 J_o \epsilon l[A] = \frac{2.303 J_o \epsilon l}{N_A h\nu} \left( \frac{A}{V} \right) [A] \quad (\epsilon l[A] \ll 1) \quad 5.1.10$$

The rate of primary photoproduction, Eq. 5.1.8, simplifies to a first-order rate law:

$$\frac{d[A^*]}{dt} = J_a = 2.303 J_o \epsilon l[A] \quad (\epsilon l[A] \ll 1) \quad 5.1.11$$

The absorbance can be small because the concentration of absorbing species is small, the molar absorption coefficient is small, or the path length is short. Because of the relationship to path length, a gas or solution with small absorbance, for whatever reason, is often called **optically thin**. A system with  $\epsilon l[A] \gg 1$  is called **optically thick**.

Now consider a photochemical reaction. Let the concentration of the photoproduct of interest be [B]. The total moles of photons per liter per second that are absorbed is  $J_a$ . Then the quantum yield for the production of B is given by:

$$\Phi_B = \frac{d[B]/dt}{J_a} \quad \text{or rearranging} \quad \frac{d[B]}{dt} = \Phi_B J_a \quad 5.1.12$$

The rate law for the formation of B is then given by substituting Eq. 5.1.7 into Eq. 5.1.12:

$$\frac{d[B]}{dt} = \Phi_B J_a = \Phi_B J_o (1 - e^{-2.303 \epsilon l[A]}) \quad 5.1.13$$

This last equation can also be simplified for optically thick and optically thin systems. If the system is optically thick,  $\epsilon l[A] \gg 1$ , all incident light is absorbed:

$$\frac{d[B]}{dt} = \Phi_B J_a = \Phi_B J_o \quad (\text{optically thick, } \epsilon l[A] \gg 1) \quad 5.1.14$$

giving zeroth-order kinetics. For optically thin systems, using Eq 5.1.10 and Eq. 5.1.12:

$$\frac{d[B]}{dt} = \Phi_B J_a = 2.303 J_o \Phi_B \epsilon l [A] \quad (\text{optically thin, } \epsilon l [A] \ll 1) \quad 5.1.15$$

giving first-order kinetics. Eqs. 5.1.11 and 5.1.15 are often useful approximations for gas phase atmospheric chemistry and for aquatic environmental applications at a narrow range of depths (a thin layer).

Eq. 5.1.11 and Eq. 5.1.15 are in the same form, a constant multiplied by the concentration of A. We can write simply for the primary photoproduct:

$$\frac{d[A^*]}{dt} = J_a = j_{A^*} [A] \quad (\text{optically thin, } \epsilon l [A] \ll 1) \quad 5.1.16$$

and for the product of a photochemical reaction:

$$\frac{d[B]}{dt} = \Phi_B J_a = j_B [A] \quad (\text{optically thin, } \epsilon l [A] \ll 1) \quad 5.1.17$$

where  $j_{A^*}$  is the rate constant for production of the excited state, and  $j_B$  is the rate constant for the photolytic production of B. The effective photolytic rate constants,  $j_{A^*}$  and  $j_B$ , are defined by Eqs. 5.1.16 and 5.1.17, in comparison with Eqs. 5.1.11 and 5.1.15, and are measured constants at a given incident light intensity:

$$j_{A^*} = 2.303 J_o \epsilon l \quad (\text{optically thin, } \epsilon l [A] \ll 1) \quad 5.1.18$$

$$j_B = \Phi_B j_{A^*} = 2.303 J_o \Phi_B \epsilon l \quad (\text{optically thin, } \epsilon l [A] \ll 1) \quad 5.1.19$$

Often a “k” is used instead of a “j” for the photolytic rate constant, which highlights the similarity between chemical and photolytic processes. The importance of Eqs. 5.1.16 and 5.1.17 is the similarity to first-order purely chemical processes, which means that we can use all the kinetics tools that we have already developed. The first step in the  $H_2 + Br_2$  chain reaction is one example; Eqs. 4.3.3 and 4.3.16 hold for thermal and photolytic processes with j’s or k’s. For another more general example, the steady-state approximation can be very useful for analyzing photolytic processes.

*With the Light On: For Rapid Deactivation, a Photochemical Process Reaches a Steady-State:*

What factors determine the value of the photochemical quantum yield? During photolysis, Eq. 5.1.16 gives the rate of production of the primary photoproduct as an excited molecular state. Once the primary excited state is formed many processes compete for the excited state, Figure 5.1.1. Let the rate constant for fluorescence be  $k_f$ , the rate constant for intersystem crossing to form the phosphorescent state be  $k_{ISC}$ , and the rate constant for non-radiative collisional processes be  $k_{nr}$ . Chemical reactions also decrease the concentration of the excited state. Assume that the rate law for the chemical reaction from the excited state is first-order,  $A^* \rightarrow B$ , or pseudo first-order:

$$\frac{d[B]}{dt} = k_R [A^*] \quad 5.1.20$$

with  $k_R$  the rate constant for the formation of a secondary photoproduct B, where the R symbolizes a chemical reaction from the excited state. Then the rate law for  $A^*$  is given by:

$$\frac{d[A^*]}{dt} = j_{A^*} [A] - k_f [A^*] - k_{ISC} [A^*] - k_{nr} [A^*] - k_R [A^*] \quad 5.1.21$$

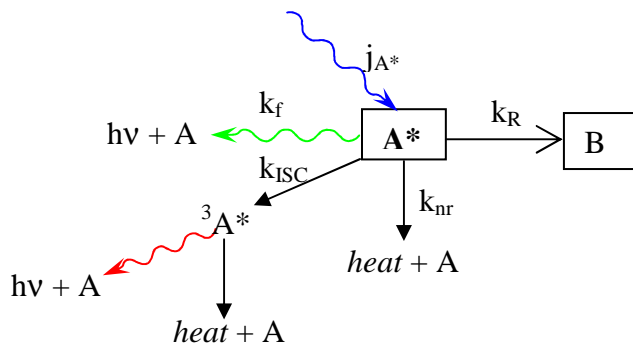


Figure 5.1.1: Many processes compete for the excited state. The symbol  ${}^3A^*$  indicates the phosphorescent state of the molecule, which can emit light as phosphorescence or lose energy by non-radiative collisional processes.

If the rate of the deactivation processes is fast compared to the rate of formation of the excited state, we can treat the excited state as a reactive intermediate using the steady-state approximation. Setting Eq. 5.1.21 equal to zero then gives the steady-state concentration of the excited state as:

$$[A^*] = \frac{j_{A^*}[A]}{k_f + k_{ISC} + k_{nr} + k_R} \quad (\text{steady state}) \quad 5.1.22$$

The rate of formation of the secondary photoproduct B is then obtained by substituting Eq. 5.1.22 into Eq. 5.1.20:

$$\frac{d[B]}{dt} = k_R [A^*] = \frac{k_R j_{A^*} [A]}{k_f + k_{ISC} + k_{nr} + k_R} \quad (\text{steady state}) \quad 5.1.23$$

The quantum yield for the chemical reaction using Eqs. 5.1.12, 5.1.16 for  $J_a$ , and 5.1.23 is:

$$\Phi_B = \frac{d[B]/dt}{J_a} = \frac{k_R}{k_f + k_{ISC} + k_{nr} + k_R} \quad (\text{steady state}) \quad 5.1.24$$

In other words, the first-order photochemical production of B is in competition with all processes that deactivate the primary photoproduct. This quantum yield can then be used in Eqs. 5.1.17 and 5.1.19 to determine the rate law for the photolytic production of the substance. If the photoproduct is produced in one elementary step from the excited state, the quantum yield is necessarily less than 100%,  $\Phi_B < 1$ . On the other hand, the  $H_2 + Br_2$  reaction, Eqs. 4.3.3-4.3.7, is an example of a chain reaction where the initial production of the reactive intermediate is amplified by the chain process. For chain and other autocatalytic reactions the photochemical quantum yield can be much larger than one. The photochemical quantum yields for natural systems vary greatly. For example, the practical limiting quantum efficiency for photosynthesis is about 20%.<sup>2,3</sup>

We can also use Eq. 5.1.22 to determine the fluorescence quantum yield. The fluorescence light flux is given by just the second term in Eq. 5.1.21,  $J_f = k_f [A^*]$ . Using Eqs. 5.1.4, 5.1.16 for  $J_a$ , and 5.1.22 then gives the fluorescence quantum yield as:

$$\Phi_f = J_f/J_a = \frac{k_f}{k_f + k_{ISC} + k_{nr} + k_R} \quad (\text{steady state}) \quad 5.1.25$$

which is in direct analogy with Eq. 5.1.24. Fluorescence and any chemical reactions compete for the molecular excited state; chemical reactions decrease the intensity of fluorescence. A chemical process that decreases the fluorescence quantum yield gives rise to **fluorescence quenching**.

Consider the reaction from the excited state:



where Q is called the **quencher** and  $k_q$  is the rate constant for the quenching process. Quenching may be treated as pseudo-first-order, since the concentration of the excited state is small and by comparison the quencher is in large excess. The reaction is pseudo-first-order with  $k_R = k_q[Q]$  and the fluorescence quantum yield from Eq. 5.1.25 is then:

$$\Phi_f = J_f/J_a = \frac{k_f}{k_f + k_{ISC} + k_{nr} + k_q[Q]} \quad (\text{pseudo-first-order, steady state}) \quad 5.1.27$$

This quenching mechanism is called the **Stern-Volmer** mechanism. Non-radiative processes can also have a concentration dependent term, which is handled identically to quenching by chemical reactions. Concentration dependent non-radiative and chemical reaction quenching are indistinguishable from fluorescence measurements alone. If  $\Phi_o$  is the quantum yield without quencher present,  $[Q] = 0$ , then the relative quantum yield is defined by the ratio:

$$\Phi_o/\Phi_f = \frac{k_f + k_{ISC} + k_{nr} + k_q[Q]}{k_f + k_{ISC} + k_{nr}} = 1 + \frac{k_q[Q]}{k_f + k_{ISC} + k_{nr}} \quad 5.1.28$$

The relative quantum yield can be replaced by the relative fluorescence flux or relative intensity, giving  $\Phi_o/\Phi_f = J_o/J_f = I_o/I$ . A plot of  $I_o/I$  versus  $[Q]$  gives a straight line with slope  $k_q/(k_f+k_{ISC}+k_{nr})$ . The quenching rate constant can be calculated if the other rate constants can be separately determined, which we discuss next.

The previous results assumed that the photolysis was on-going; the light was on. What happens after the light source is turned off?

*With the Light Off: First-Order Competitive Processes Deactivate the Excited State:* The rate law after the light is turned off is simply Eq. 5.1.21 without the excited state production term:

$$\frac{d[A^*]}{dt} = -k_f[A^*] - k_{ISC}[A^*] - k_{nr}[A^*] - k_R[A^*] \quad 5.1.29$$

The deactivation process is a first-order parallel or competitive mechanism. Then by Eq. 4.1.6:

$$[A^*] = [A^*]_o e^{-(k_f + k_{ISC} + k_{nr} + k_R)t} \quad 5.1.30$$

where  $[A^*]_o$  is the steady-state concentration of the excited state when the excitation source is turned off. The lifetime of the excited state can then be found using Eq. 4.1.15:

$$\frac{1}{\tau} = k_f + k_{ISC} + k_{nr} + k_R = \frac{1}{\tau_f} + \frac{1}{\tau_{ISC}} + \frac{1}{\tau_{nr}} + \frac{1}{\tau_R} \quad 5.1.31$$

where  $\tau_f = 1/k_f$  is the **intrinsic fluorescence lifetime** in the absence of any competing processes. Similarly,  $\tau_{ISC} = 1/k_{ISC}$  is the lifetime for intersystem crossing to the phosphorescent state, with

analogous definitions for the remaining terms. How can the lifetime of the excited state,  $\tau$ , be measured?

The observed lifetime,  $\tau$ , in Eq. 5.1.31 is determined using pulsed fluorescence measurements. The fluorescence intensity is given by just the first term in Eq. 5.1.29,  $J_f = k_f [A^*]$ . The light flux or intensity of fluorescence is then given using Eq. 5.1.30 as:

$$J_f = k_f [A^*] = k_f [A^*]_0 e^{-(k_f + k_{ISC} + k_{nr} + k_R) t} = k_f [A^*]_0 e^{-t/\tau} \quad 5.1.32$$

The observed fluorescence lifetime,  $\tau$ , is the excited state lifetime and is determined as the exponential time constant for the intensity of fluorescence following a short pulse of light. Note that the corresponding equation from Chapter 3, Eq. 3.2.11, gives  $k_f^*$  as the sum of the rate constants for all the competing processes;  $k_f^* = k_f + k_{ISC} + k_{nr} + k_R$ .

In a Stern-Volmer quenching study, based on Eq. 5.1.28, the quenching rate constant  $k_q$  can be determined if  $k_f + k_{ISC} + k_{nr}$  is known. The sum of these rate constants can be determined by a lifetime determination in the absence of the quencher, that is when  $k_R = k_q[Q] = 0$ . Using Eq. 5.1.32, in the absence of quencher the lifetime is given using  $k_R = k_q[Q] = 0$ :

$$\frac{1}{\tau} = k_f + k_{ISC} + k_{nr} \quad ([Q] = 0) \quad 5.1.33$$

### Example 5.1.1:

Argon ion lasers produce intense blue light at 488 nm that is commonly used for photochemical experiments (and for tattoo removal).<sup>4</sup> The output from a 0.120 W laser is expanded to a 1.00 cm<sup>2</sup> cross-sectional area beam to irradiate a 5.00-cm path length reaction cell. The yellow dye, sodium fluorescein, photobleaches to produce a colorless product. The reaction cell is filled with 10.00 mL of a 1.33x10<sup>-6</sup> M solution. The molar extinction coefficient is 9170. M<sup>-1</sup> cm<sup>-1</sup>.<sup>5</sup> Calculate the initial rate of production of the colorless product, assuming a quantum yield of 2.20x10<sup>-5</sup>.

*Answer:* The plan is to calculate the light flux in J s<sup>-1</sup> m<sup>-2</sup>, the energy per mole of photons at 488 nm, and then use Eq. 5.1.19 to find the photochemical rate constant assuming an optically thin solution. The incident flux is given by the laser power divided by the beam area:

$$J_0 = P/A = 0.120 \text{ W}/1.00 \text{ cm}^2 (100 \text{ cm}/1 \text{ m})^2 = 1.20 \times 10^3 \text{ W m}^{-2} = 1.20 \times 10^3 \text{ J s}^{-1} \text{ m}^{-2}$$

The energy of 488 nm light is given by  $E = hv = hc/\lambda$ :

$$E = \frac{6.626 \times 10^{-34} \text{ J s} (2.998 \times 10^8 \text{ m s}^{-1})}{488 \times 10^{-9} \text{ m}} = 4.071 \times 10^{-19} \text{ J per photon}$$

or alternatively per mole of photons:  $E = N_A hv = 2.451 \times 10^5 \text{ J mol}^{-1} = 245.1 \text{ kJ mol}^{-1}$ .

Then  $j_B$  is given by Eqs. 5.1.6 and 5.1.19, assuming an optically thin solution:

$$j_B = \left( \frac{2.303 J_0 \epsilon \ell \Phi_B}{N_A hv} \right) \left( \frac{A}{V} \right) \quad \text{with } \ell \text{ in cm, } A \text{ in m}^2, \text{ and } V \text{ in L}$$

$$= \left( \frac{2.303 (1.20 \times 10^3 \text{ J s}^{-1} \text{ m}^{-2})(9170. \text{ M}^{-1} \text{ cm}^{-1})(5.00 \text{ cm})(2.20 \times 10^{-5})}{2.451 \times 10^5 \text{ J mol}^{-1}} \right) \left( \frac{1 \text{ cm}^2 (1 \text{ m}/100 \text{ cm})^2}{0.0100 \text{ L}} \right)$$

$$= 1.137 \times 10^{-4} \text{ s}^{-1}$$

and finally the initial rate of photobleaching is from Eq. 5.1.17:

$$\frac{d[B]}{dt} = j_B [A] = 1.137 \times 10^{-4} \text{ s}^{-1} (1.33 \times 10^{-6} \text{ M}) = 1.51 \times 10^{-10} \text{ M s}^{-1}$$

### Example 5.1.2:

Show that the photochemical quantum yield can also be expressed as  $\Phi_B = n_B/n_{\text{photons}}$ , where  $n_B$  is the number of moles of photoproduct and  $n_{\text{photons}}$  is the number of moles of photons absorbed in a given time period,  $\Delta t$ .

*Answer:* Assume the solution volume is  $V$  and the time interval for the measurement is  $\Delta t$ . The moles of product formed is given by:

$$n_B = \frac{d[B]}{dt} V \Delta t \quad 5.1.34$$

The moles of absorbed photons in time  $\Delta t$  is given by:

$$n_{\text{photons}} = J_a V \Delta t \quad 5.1.35$$

since the units of  $J_a$  are  $\text{mol L}^{-1} \text{ s}^{-1}$ . Multiplying Eq. 5.1.12 by  $V \Delta t$  in the numerator and denominator and using Eqs. 5.1.33 and 5.1.34 gives:

$$\Phi_B = \frac{\frac{d[B]}{dt} V \Delta t}{J_a V \Delta t} = n_B/n_{\text{photons}} \quad 5.1.36$$

The quantum yield can be calculated using any property that is proportional to these quantities, as long as the units match in the numerator and denominator.

## 5.2 Stratospheric Ozone Depletion - Simulating Complex Mechanisms Requires Special Numerical Techniques

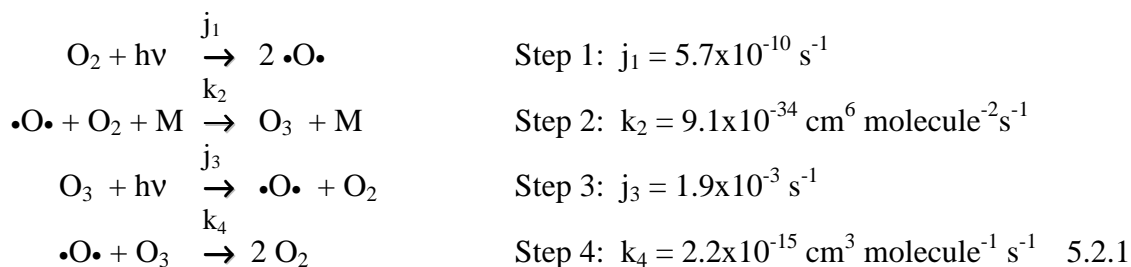
Understanding biogeochemical cycles, the fate of environmental pollutants, photosynthesis, metabolism, and other complex chemical phenomena requires the integration of the rate laws for complex multi-step mechanisms. As we mentioned in Sec. 4.1, the finite difference approximation is used for this purpose. However, a practical problem arises if the rate constants for the different mechanistic steps span multiple orders of magnitude. In principle, one simply needs to choose the time increment  $\Delta t$  such that  $\Delta t \ll 1/k$  for the largest rate constant. However, in practice, such a small time increment requires too much computer time to be practical when the simulation is extended to the total times that are necessary for understanding all the coupled chemical phenomena of such complicated systems. At first this issue may seem trivial; however, billions of dollars in public and private investments often depend on the results of these chemical models. Models on the production and fate of environmental pollutants, especially ozone, are necessary to inform public policy decisions on legislation for amelioration strategies. The global warming debate is informed by global environmental models for  $\text{CO}_2$  production, dispersion, and



consumption by photosynthetic processes in forests and the oceans. Drug design strategies are informed by models of complex enzyme-mediated pathways in the progression of human diseases. Chemical kinetics is one of those scientific areas that has a direct and immediate impact on the proper functioning of our society. Luckily, however, the underlying theory of differential equations is well developed, since differential equations are so broadly used in many different fields, including engineering, economics, financial markets, and all the sciences.

Differential equation models that involve time scales over multiple orders of magnitude are called **stiff models**. One of the ways that stiff models are solved is to vary the time increment,  $\Delta t$ , during the course of the simulation, using short increments when concentrations are changing rapidly and long increments when concentrations are changing slowly. Efficient algorithms have also been developed that use matrix methods to accurately solve large systems of simultaneous differential equations. Applications like *MatLab* and *MathCad* and environmental modeling programs have routines specifically designed for these purposes. All we need to do is to express our mechanisms in a specific matrix format to take advantage of these advanced techniques.

*Stratospheric Ozone Depletion:* The Chapman ozone mechanism is an excellent example for the discussion of numerical integration. The Chapman mechanism is a cyclic free radical chain mechanism that is active in the stratosphere.<sup>6</sup> If we focus only on oxygen-containing species, the mechanism for the production and destruction of ozone is:



The direct photolysis of  $\text{O}_2$  in step 1 produces a ground state O atom, here depicted as  $\bullet\text{O}\bullet$  to show its triplet character, and an excited state O atom. However, the excited state rapidly converts through collisions to the ground state. (The excited state O atom is also consumed in other atmospheric processes.) The M in the second step is any third body, which includes all atmospheric constituents. For gas phase associations, such as step 2, the third body is necessary to carry away excess energy after the collision. Otherwise, because of conservation of energy, the single product is too energetic, and immediately dissociates back to reactants. The concentration units are number densities in molecules  $\text{cm}^{-3}$ , since molar concentrations would be so small. The rate constants are appropriate for an altitude in the stratosphere of 40 km.<sup>7</sup>

---

#### Example 5.2.1:

Ozone and O atoms ( $\bullet\text{O}\bullet$ ) are rapidly interconverted by steps 2 and 3 to give a net pool of reactive species and so are often lumped together. The concentration of **odd oxygen** species in the atmosphere is then given by  $([\text{O}_3] + [\text{O}])$ , where  $[\text{O}]$  is the concentration of ground state  $\bullet\text{O}\bullet$ . Use the steady-state approximation to find the steady-state concentration of odd oxygen species from the Chapman mechanism at 40 km. Typical concentrations are  $[\text{M}] = 8.1 \times 10^{16}$  molecules  $\text{cm}^{-3}$  and  $[\text{O}_2] = 1.7 \times 10^{16}$  molecules  $\text{cm}^{-3}$ .

*Answer:* Assuming steps 1 and 3 are optically thin, the rate laws are given as:

$$\frac{d[\text{O}]}{dt} = 2 j_1 [\text{O}_2] - k_2 [\text{O}][\text{O}_2][\text{M}] + j_3 [\text{O}_3] - k_4 [\text{O}][\text{O}_3] \quad 5.2.2$$

$$\frac{d[\text{O}_2]}{dt} = -j_1 [\text{O}_2] - k_2 [\text{O}][\text{O}_2][\text{M}] + j_3 [\text{O}_3] + 2 k_4 [\text{O}][\text{O}_3] \quad 5.2.3$$

$$\frac{d[\text{O}_3]}{dt} = k_2 [\text{O}][\text{O}_2][\text{M}] - j_3 [\text{O}_3] - k_4 [\text{O}][\text{O}_3] \quad 5.2.4$$

The rate of formation of odd oxygen species is obtained by adding Eqs. 5.2.2 and 5.2.4 to give:

$$\frac{d([\text{O}_3] + [\text{O}])}{dt} = \underbrace{2 j_1 [\text{O}_2]}_{\text{production}} - \underbrace{2 k_4 [\text{O}][\text{O}_3]}_{\text{destruction}} \quad 5.2.5$$

Steps 2 and 3 are chain propagation steps that operate in a cycle. Since 2 and 3 are the reverse of each other from the perspective of  $\text{O}_3$  and  $\bullet\text{O}\bullet$  atoms, at steady state steps 2 and 3 don't change the net amount of  $\text{O}_3$  or  $\bullet\text{O}\bullet$  atoms. The net rate into this reversible pair represents the rate of production of ozone and the net rate out of the reversible pair represents the rate of destruction of ozone. The rate of production of ozone is then given by step 1,  $\nu_{\text{pr}} = 2 j_1 [\text{O}_2]$ , and the rate of destruction of ozone is given by step 4,  $\nu_{\text{des}} = 2 k_4 [\text{O}][\text{O}_3]$ . We can consider the  $\bullet\text{O}\bullet$  atoms as the reactive intermediate. Applying the steady-state approximation to the  $\bullet\text{O}\bullet$  atoms from Eq. 5.2.2:

$$2 j_1 [\text{O}_2] - k_2 [\text{O}][\text{O}_2][\text{M}] + j_3 [\text{O}_3] - k_4 [\text{O}][\text{O}_3] = 0 \quad (\text{steady state}) \quad 5.2.6$$

$$\text{gives } [\text{O}] = \frac{2 j_1 [\text{O}_2] + j_3 [\text{O}_3]}{k_2 [\text{O}_2][\text{M}] + k_4 [\text{O}_3]} \quad (\text{steady state}) \quad 5.2.7$$

and substituting into Eq. 5.2.5 for  $[\text{O}]$  gives:

$$\frac{d([\text{O}_3] + [\text{O}])}{dt} = 2 j_1 [\text{O}_2] - 2 k_4 [\text{O}_3] \frac{2 j_1 [\text{O}_2] + j_3 [\text{O}_3]}{k_2 [\text{O}_2][\text{M}] + k_4 [\text{O}_3]} \quad (\text{steady state}) \quad 5.2.8$$

As in Eq. 5.2.5, the first term represents the production of ozone and the second term the destruction. Now, also assuming steady state for ozone as well as O atoms, we set Eq. 5.2.8 equal to zero and then:

$$2 j_1 [\text{O}_2] = 2 k_4 [\text{O}_3] \frac{2 j_1 [\text{O}_2] + j_3 [\text{O}_3]}{k_2 [\text{O}_2][\text{M}] + k_4 [\text{O}_3]} \quad (\text{steady state}) \quad 5.2.9$$

Cross multiplying and rearranging gives:

$$2 j_3 k_4 [\text{O}_3]^2 + 2 j_1 k_4 [\text{O}_2] [\text{O}_3] - 2 j_1 k_2 [\text{O}_2]^2 [\text{M}] = 0 \quad (\text{steady state}) \quad 5.2.10$$

Solving the quadratic equation gives:

$$[\text{O}_3] = \frac{(-2 j_1 k_4 [\text{O}_2] \pm \sqrt{(2 j_1 k_4 [\text{O}_2])^2 + 16 j_1 k_2 j_3 k_4 [\text{O}_2]^2 [\text{M}]})}{4 j_3 k_4} \quad (\text{steady state}) \quad 5.2.11$$

Only the positive root gives a positive ozone concentration with  $[\text{O}_3] = 1.7 \times 10^{12} \text{ molecule cm}^{-3}$ .

To simulate the time dependence of the Chapman model, we need to recast the differential equations into a vector form. The concentrations of all species are arranged as a vector:

$$\tilde{X} = \begin{pmatrix} [X_1] \\ [X_2] \\ [X_3] \end{pmatrix} = \begin{pmatrix} [O] \\ [O_2] \\ [O_3] \end{pmatrix} \quad 5.2.12$$

The differential equations for each species, which are functions of  $t$  and  $\tilde{X}$ , are also arranged as a vector. Eqs. 5.2.2-5.2.4 are rewritten as:

$$\tilde{D}(t, \tilde{X}) = \begin{pmatrix} 2 j_1 [X_2] - k_2 [M][X_1][X_2] + j_3 [X_3] - k_4 [X_1][X_3] \\ - j_1 [X_1] - k_2 [M][X_1][X_2] + j_3 [X_3] + 2 k_4 [X_1][X_3] \\ k_2 [M][X_1][X_2] - j_3 [X_3] - k_4 [X_1][X_3] \end{pmatrix} \quad 5.2.13$$

The initial conditions, in units of molecules  $\text{cm}^{-3}$ , are chosen as:

$$[\tilde{X}]_o = \begin{pmatrix} [O]_o \\ [O_2]_o \\ [O_3]_o \end{pmatrix} = \begin{pmatrix} 0 \\ 1.7 \times 10^{16} \\ 0 \end{pmatrix} \quad 5.2.14$$

The *MatLab* files for this problem are listed in Addendum 5.7. The results are shown in Figure 5.2.1.

The simulation results give the same steady-state ozone concentration as Example 5.2.1. The Chapman mechanism is a good example of photochemical environmental applications. However, reaction mechanisms can also involve interactions on surfaces. In particular, heterogeneous catalysis on surfaces can play an important role in environmental and industrial processes.

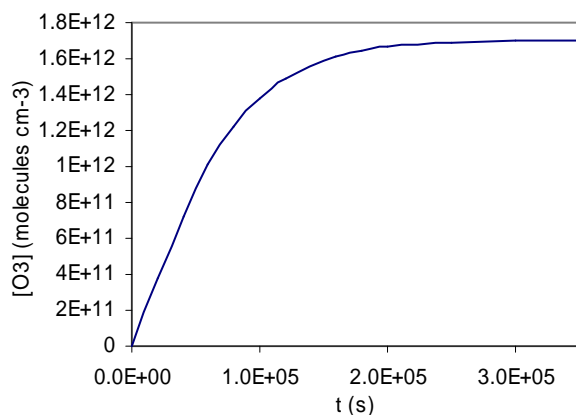


Figure 5.2.1: Ozone concentration for the Chapman mechanism at an altitude of 40 km. The initial  $O_2$  concentration was set at  $1.7 \times 10^{16}$  molecules  $\text{cm}^{-3}$ .

### 5.3 Chemical Species Can Adsorb on Surfaces

The adsorption of molecules from the gas phase or solution onto surfaces plays an important role in understanding the partitioning of substances in heterogeneous environments. Applications include understanding the fate and transport of environmental contaminants and heterogeneous catalysis. Adsorption on a surface can be described along a continuum between two extremes.

**Physical adsorption** is the rapid and reversible interaction of a substance with a surface through non-covalent forces, such as hydrogen-bonding, dipolar forces, and dispersion forces. The

strength of physical adsorption interactions is typically less than  $20 \text{ kJ mol}^{-1}$ . **Chemical adsorption** involves the formation of covalent bonds to surface atoms or strong ionic interactions. The interaction energy is on the order of the strength of typical covalent bonds, which is often greater than  $200 \text{ kJ mol}^{-1}$ . Chemical adsorption and desorption are usually much slower than physical adsorption. **A**bsorption is distinct from adsorption; **a**bsorption occurs when molecules fill voids in a porous surface. **A**dsorption involves a direct interaction with the surface atoms, while **a**bsorption does not. Surface adsorption is readily described using kinetic arguments with the introduction of the concept of surface concentration and noticing that adsorption sites on the surface are often the “limiting reagent.”

Applications of surface adsorption are often in circumstances where the adsorbate is very dilute or in consideration of surface catalysis where only the layer of adsorbate directly adjacent to the surface is catalytically active. Therefore, we restrict our treatment to the description of the formation of a **monolayer** of adsorbate on a solid surface. The resulting equation is often applicable for gas phase and solution species; however, for ease of argument we first consider gas phase interactions. The **surface concentration** of species A on the surface is defined as  $[A]_{\sigma} \equiv n_{A\sigma}/\sigma$ , where  $n_{A\sigma}$  is the number of moles of A bound to the surface and  $\sigma$  is the surface area. Surfaces have a maximum capacity for adsorption. Define the surface concentration of the free binding sites as  $[B]_{\sigma} \equiv n_{B\sigma}/\sigma$ , where  $n_{B\sigma}$  is the number of moles of free binding sites on the surface. The maximum concentration of binding sites on the surface is given as  $[B]_{0\sigma} \equiv n_{B0}/\sigma$ , where  $n_{B0}$  is the total moles of binding sites. The mole balance between free and occupied sites is given by:

$$[B]_{0\sigma} = [B]_{\sigma} + [A]_{\sigma} \quad 5.3.1$$

The surface concentration has units of  $\text{mol m}^{-2}$ . Since the surface area of the solid is often small compared to the total reaction volume, the number of binding sites is usually the limiting reagent in the interaction. The maximum surface concentration for A is equal to the total concentration of binding sites on the surface,  $[A]_{\text{max}\sigma} = n_{A\text{max}}/\sigma = [B]_{0\sigma}$ . The **fractional coverage** of A on the surface,  $\theta_A$ , is given by the ratio:

$$\theta_A = \frac{[A]_{\sigma}}{[A]_{\text{max}\sigma}} = \frac{n_{A\sigma}/\sigma}{n_{A\text{max}}/\sigma} = \frac{n_{A\sigma}}{n_{A\text{max}}} \quad 5.3.2$$

The surface concentration of A can readily be obtained from  $\theta_A$  by rearranging this last equation:

$$[A]_{\sigma} = [A]_{\text{max}\sigma} \theta_A = [B]_{0\sigma} \theta_A \quad 5.3.3$$

The surface coverage can be visualized using a model of the surface as containing fixed adsorption sites, Figure 5.3.1. The fraction of occupied sites is  $\theta_A$ , and the fraction of adsorption sites that are free is  $(1 - \theta_A)$ .

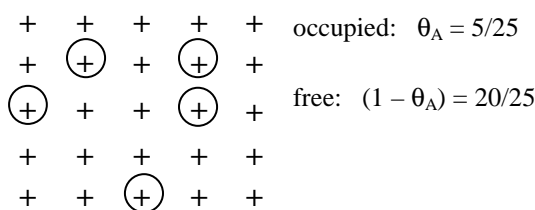


Figure 5.3.1: Binding sites can be occupied or free. The fraction of free sites is  $(1 - \theta_A)$ .

The mechanism for surface adsorption can be approximated by a second-order forward process, where a gas molecule combines with a free site. The desorption is a first-order reverse process:



where  $B_{\sigma}$  is a free binding site on the surface,  $A_{\sigma}$  is the adsorbed species,  $k_a$  is the rate constant for adsorption, and  $k_d$  is the rate constant for desorption. We assume all sites are equivalent and that the probability a site is occupied is independent of the occupancy of adjacent sites. With these assumptions, the rate law for the process in terms of the surface concentration is given by:

$$\frac{d[A]_{\sigma}}{dt} = k_a[B]_{\sigma}P_A - k_d[A]_{\sigma} \quad 5.3.5$$

where  $P_A$  is the partial pressure of A in the gas phase. Using Eq. 5.3.3 for the surface concentration of A and the corresponding equation for the free sites gives:

$$\frac{d[A]_{\sigma}}{dt} = k_a[B]_{o\sigma}(1 - \theta_A)P_A - k_d[B]_{o\sigma}\theta_A \quad 5.3.6$$

Dividing this last equation by the maximum surface concentration,  $[A]_{\max\sigma}$  or equivalently  $[B]_{o\sigma}$ , gives the rate law for the fractional coverage:

$$\frac{d\theta_A}{dt} = k_a(1 - \theta_A)P_A - k_d\theta_A \quad 5.3.7$$

At equilibrium, the rate of change of the fractional coverage is zero:

$$\frac{d\theta_A}{dt} = k_a(1 - \theta_A)P_A - k_d\theta_A = 0 \quad (\text{equilibrium}) \quad 5.3.8$$

Solving for the fractional coverage at equilibrium gives:

$$\theta_A = \frac{k_a P_A}{k_d + k_a P_A} \quad (\text{equilibrium}) \quad 5.3.9$$

This equation is called the Langmuir adsorption isotherm. The equilibrium constant for the process based on Eq. 5.3.4 is defined as:

$$b \equiv \frac{k_a}{k_d} \quad 5.3.10$$

Dividing the numerator and denominator of Eq. 5.3.9 by  $k_d$  and using this definition gives:

$$\theta_A = \frac{b P_A}{1 + b P_A} \quad (\text{equilibrium}) \quad 5.3.11$$

which is the form of the Langmuir adsorption isotherm most often found in the literature.

Notice the limiting behavior of Eq. 5.3.11. For low partial pressures or weak binding, which corresponds to small  $b$ , the  $bP_A$  term in the denominator can be neglected and the Langmuir isotherm reduces to:

$$\theta_A = b P_A \quad (\text{equilibrium, small } P_A \text{ or } b) \quad 5.3.12$$

In other words, the surface coverage is a linear function of the partial pressure. For large partial pressures of the adsorbate or for very strong adsorption, which corresponds to large  $b$ :

$$\theta_A \approx 1 \quad (\text{equilibrium, large } P_A \text{ or } b) \quad 5.3.13$$

In other words for high partial pressures of adsorbate, the surface coverage reaches a maximum at 100%. The fraction of the surface area that is free, that is not occupied by A, is given by:

$$1 - \theta_A = \frac{1}{1 + b P_A} \quad (\text{equilibrium}) \quad 5.3.14$$

The fraction of the surface area that is free is often important since other molecules can then gain access to the surface. For high partial pressures of A or strong binding, the “1” in the denominator is small compared to  $bP_A$  and this last equation can be approximated as:

$$1 - \theta_A = \frac{1}{b P_A} \quad (\text{equilibrium, large } P_A \text{ or } b) \quad 5.3.15$$

The Langmuir  $b$  coefficient is best determined by non-linear curve fitting to Eq. 5.3.11. However, Langmuir type behavior is often verified by a double reciprocal plot based on the inverse of Eq. 5.3.11:

$$\frac{1}{\theta_A} = \frac{1 + b P_A}{b P_A} = \frac{1}{b P_A} + 1 \quad (\text{equilibrium}) \quad 5.3.16$$

In an analogous fashion to the Lineweaver-Burke plot for the Michaelis-Menten mechanism, a plot of  $1/\theta_A$  versus  $1/P_A$  gives straight line with a slope of  $1/b$ . Adsorption onto surfaces can follow other relationships, depending on the circumstances. For example, Langmuir behavior does not hold for adsorption of multiple layers. However, Langmuir behavior is quite commonly observed. A particularly important application is to biomolecular interaction analysis, or BIA. Another important application of the Langmuir adsorption isotherm is to heterogeneous catalysis.

---

#### Example 5.3.1:

Phosphate is a necessary nutrient for plant and animal growth. Phosphate is often the limiting nutrient in aquatic ecosystems. Free  $\text{HPO}_4^{2-}$  and  $\text{H}_2\text{PO}_4^-$  (*ortho*-phosphate) readily adsorb on particle surfaces, which decreases the bio-availability. Adsorption on alumina,  $\text{Al}_2\text{O}_3$ , is a good model system for some types of particulates in natural waters.<sup>8</sup> The data table, below, lists the equilibrium loading in  $\mu\text{mol}$  of phosphate per gram,  $\Gamma$ , of alumina for varying phosphate concentrations. The phosphate concentrations are listed in  $\mu\text{-molar}$  units. Calculate the Langmuir binding coefficient,  $b$ .

$[\text{H}_2\text{PO}_4^-]$ ( $\mu\text{M}$ )	1	3.2	5	18	33	58	85
$\Gamma$ ( $\mu\text{mol g}^{-1}$ )	4	10	23	30	34	37	40

*Answer:* We need to make some comments about units. First, since we are working in solution, the partial pressure is replaced by the concentration of the adsorbate. Starting with Eq. 5.3.11 and using Eq. 5.3.3 for the surface concentration of adsorbate gives:

$$[A]_{\sigma} = [B]_{\sigma} \frac{b [A]}{1 + b [A]} \quad (\text{equilibrium}) \quad 5.3.17$$

However, the surface concentration of binding sites is often not known, because the active surface area is not available. Instead, the **surface loading** is used, which is the moles of surface sites per gram of solid:  $\Gamma_{A\sigma} = n_A/m$  and  $\Gamma_{\max\sigma} = n_{A\max}/m$ , where  $m$  is the mass of solid sorbent. In these units, Eq. 5.3.11 is written:

$$\Gamma_{A\sigma} = \Gamma_{\max\sigma} \frac{b P_A}{1 + b P_A} \quad (\text{equilibrium}) \quad 5.3.18$$

Based on Eq. 5.3.11 or 5.3.18, using the general form “ $abx/(1+bx)$ ” in the “Nonlinear Least Squares Curve Fitting” applet gives the results below, and corresponding curve-fit plot. Visual inspection of the curve fit, and the small relative size of the curve fit uncertainties verify Langmuir behavior with  $b = 0.151 \pm 0.037 \mu\text{M}^{-1}$ . To convert to molar units:

$$b = 0.151 \mu\text{M}^{-1} (1 \times 10^{-6} \text{ M}/1 \mu\text{M}) = 1.51 \times 10^{-7} \pm 0.37 \times 10^{-7} \text{ M}$$

The maximum surface loading is given by the a coefficient:  $41.9 \pm 2.5 \mu\text{mol g}^{-1}$ .

===== Results =====

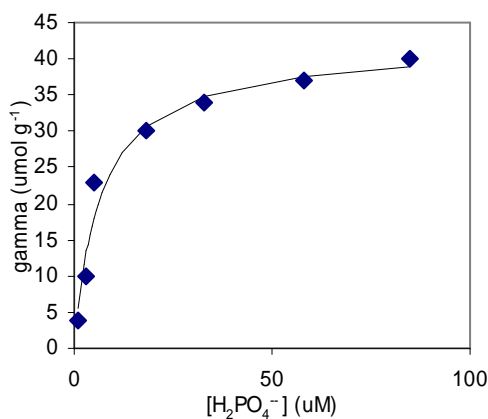
a= 41.9 +- 2.5

b= 0.151 +- 0.037

-----  
sum of squared residuals= 43.15

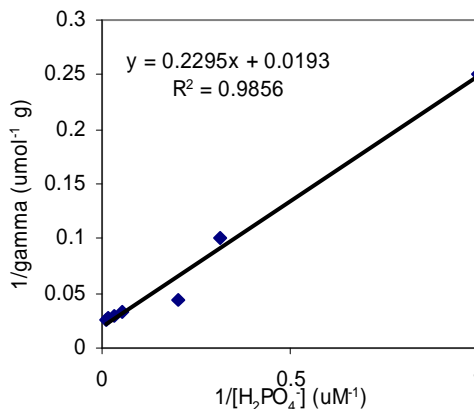
stand. dev. y values= 2.938

correlation between a & b= -0.7595



A double reciprocal plot is also commonly done, Eq. 5.3.16, but the Langmuir coefficient is better obtained from the nonlinear fit. The linear fit is determined in the following spreadsheet:

[H <sub>2</sub> PO <sub>4</sub> ] ( $\mu\text{M}$ )	$\Gamma$ ( $\mu\text{mol g}^{-1}$ )	1/[H <sub>2</sub> PO <sub>4</sub> ] ( $\mu\text{M}^{-1}$ )	1/ $\Gamma$
1	4	1	0.25
3.2	10	0.312	0.1
5	23	0.2	0.0435
18	30	0.0556	0.0333
33	34	0.0303	0.0294
58	37	0.0172	0.0270
85	40	0.0118	0.025



The general form of Eqs. 5.3.11 and 5.3.18 is quite common. We will define a *General Pattern* based on this functional form in the chapter on chemical equilibrium.

---

## 5.4 Biomolecular Recognition can be Measured Using Surface Interactions

Processes at the molecular level in living systems are controlled by biomolecular binding. For example, enzyme-substrate binding is a central issue in the proper functioning of living cells. Most drugs are designed to bind to enzymes to either enhance the activity of the enzyme or to block enzyme-substrate binding. In addition, proteins rarely act alone. Protein-protein binding is often an important control step for cellular processes. Protein-nucleic acid binding is important in many of the steps for turning genetic information into functioning cellular building blocks. The study of all these types of binding is necessary to characterize the proper functioning of the cellular machinery and to design drug intervention strategies. How do molecules recognize and bind to each other? The field of **molecular recognition** is the study of structure-function relationships in binding interactions. **Biomolecular interaction analysis** is the experimental determination of biomolecular binding rate constants and equilibrium constants.<sup>9-11</sup>

A very general and highly-sensitive technique for biomolecular interaction analysis is **surface plasmon resonance**, or **SPR**. In SPR one member of the binding pair is attached to a gold-coated surface and the other member of the pair is dissolved in a solution in contact with the surface. The molecule in solution is called the analyte or **ligand**. In SPR, and other similar surface analysis methods, surface adsorption corresponds to the specific molecular binding process. The interaction of the ligand with the surface is usually modeled using a Langmuir adsorption isotherm. The process of attaching one of the binding pair to the surface usually causes little perturbation of the binding interaction.

SPR is a very sensitive method for determining the index of refraction of surface-bound layers. The index of refraction of a surface-bound layer is proportional to the concentration of bound molecules. The index of refraction is given by the ratio of the speed of light in the sample compared to the speed of light in vacuum,  $n = v(\text{sample})/v(\text{vacuum})$ . The index of refraction of a substance is directly related to the molecular polarizability, which in turn depends in large part on molecular size. Therefore, the index of refraction is a completely general property of any molecule. However, the sensitivity increases greatly with molecular size.

SPR uses a nice trick to enhance the sensitivity of index of refraction measurements. Under suitable conditions, shining a light beam at a high incidence angle on a thin film of a metal causes the absorption of light and the production of a surface plasmon. The surface plasmon is a collective motion of the electrons near the surface of the metal. The effect is to create electron density waves that propagate along the surface. A useful analogy is to compare the motion of the electrons to the propagation of sound waves. In sound the energy of the wave is propagated in oscillating regions of high and low molecule density. Surface plasmons are similar, but with free electrons at the surface. The effect of the plasmon is to create a very strong oscillating electric field near the surface, which is called the **evanescent wave**. This electric field is greater than would have been produced by the original light beam. This enhanced electric field can interact with any molecules that are adsorbed to the surface, changing the effective propagation speed. A diagram of the geometry for the measurement is given in Figure 5.4.1. The heart of the sample cell is a thin gold film that has been deposited on a glass slide. A prism bends a monochromatic laser beam to strike the gold film at a large incidence angle (measured from the normal to the



gold surface). The light is absorbed, propagates along the gold surface as a plasmon, and then is reemitted. The light emerging from the prism has a strong dependence of intensity with angle. Light emitted at the resonance angle undergoes strong destructive interference with the input beam that creates a minimum in reflected intensity. The resonance angle is used to determine the index of refraction of the sample through a cubic calibration equation.

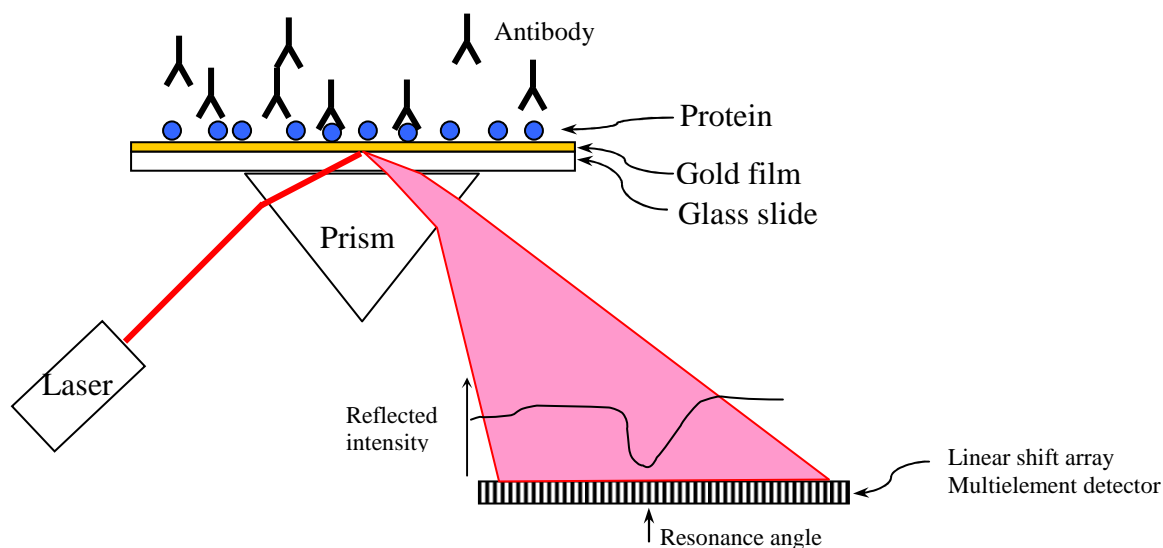


Figure 5.4.1. Geometry for surface plasmon resonance measurements. A common SPR determination is the binding of an antibody (e.g. immunoglobulin G, IgG) with an antigen.

Kinetics studies using SPR are done in two sequential steps. In the first association phase the analyte, A, is made to flow over the surface with the surface-bound molecule,  $B_{\sigma}$ . The concentration of  $AB_{\sigma}$  complex builds in a pseudo-first order process. Then in the second dissociation phase only a buffer is allowed to flow over the surface. The  $AB$  complex on the surface then dissociates to give free analyte and free bound B, Figure 5.4.2.

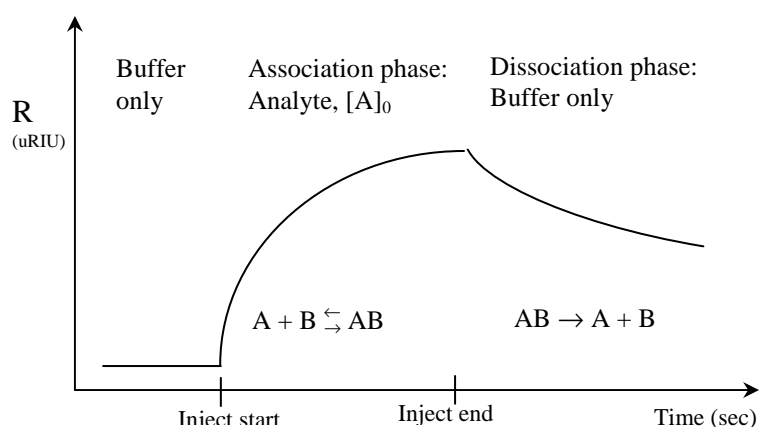


Figure 5.4.2: Kinetic time course for one value of the analyte concentration,  $[A]_0$ .

The mechanism is identical to Eq. 5.3.4, except that the adsorbate is in solution instead of the gas phase. Let  $[B]_{\sigma}$  be the concentration of the molecule bound to the surface and  $[A]$  be the solution concentration of the analyte. The surface concentration of bound complex is  $[AB]_{\sigma}$ :



The equilibrium constant for the association reaction is  $K_A = k_a/k_d$ . Medicinal chemists usually quote the dissociation equilibrium constant,  $K_D = k_d/k_a$ , which has the units of concentration. The rate law corresponding to Eq. 5.3.5 is:

$$\frac{d[AB]_{\sigma}}{dt} = k_a[A][B]_{\sigma} - k_d[AB]_{\sigma} \quad 5.4.2$$

*Association Phase:* In SPR experiments during the association phase, the analyte concentration is held constant by allowing the analyte solution to flow over the surface. Therefore,  $[A] = [A]_o$ , which is the concentration of the analyte for each individual run.  $[A]_o$  is varied over several separate experiments. The mole balance, Eq. 5.3.1, gives:

$$[B]_{o\sigma} = [B]_{\sigma} + [AB]_{\sigma} \quad 5.4.3$$

Solving for  $[AB]_{\sigma}$  gives the concentration of complex by difference:

$$[AB]_{\sigma} = [B]_{o\sigma} - [B]_{\sigma} \quad 5.4.4$$

Substitution of Eq. 5.4.4 into the rate law, Eq. 5.4.2, gives:

$$\frac{d[AB]_{\sigma}}{dt} = k_a[A]_o[B]_{\sigma} - k_d([B]_{o\sigma} - [B]_{\sigma}) \quad 5.4.5$$

Collecting terms in  $[B]_{\sigma}$  gives:

$$\frac{d[AB]_{\sigma}}{dt} = (k_a[A]_o + k_d) [B]_{\sigma} - k_d[B]_{o\sigma} \quad 5.4.6$$

Substituting mole balance Eq. 5.4.4 into the rate derivative gives the rate in terms of the concentration of free B sites:

$$\frac{d[AB]_{\sigma}}{dt} = \frac{d([B]_{o\sigma} - [B]_{\sigma})}{dt} = -\frac{d[B]_{\sigma}}{dt} \quad 5.4.7$$

which can be substituted into Eq. 5.4.6

$$-\frac{d[B]_{\sigma}}{dt} = (k_a[A]_o + k_d) [B]_{\sigma} - k_d[B]_{o\sigma} \quad 5.4.8$$

At this point several approaches may be taken. Biomolecular interactions are typically quite strong, so that  $K_A \gg 1$  giving  $k_d \ll k_a$ ; in other words, the analyte is a high affinity ligand. With this approximation, the second term in Eq. 5.4.8 is negligible giving:

$$-\frac{d[B]_{\sigma}}{dt} = (k_a[A]_o + k_d) [B]_{\sigma} \quad (k_d \ll k_a) \quad 5.4.9$$

The constants in Eq. 5.4.9 can be grouped to give an effective observed first-order rate constant:

$$k_{\text{obs}} = k_a [A]_o + k_d \quad (k_d \ll k_a) \quad 5.4.10$$

Then Eq. 5.4.9 is seen to be a simple first-order rate law:

$$-\frac{d[B]_{\sigma}}{dt} = k_{\text{obs}} [B]_{\sigma} \quad (k_d \ll k_a) \quad 5.4.11$$

The integrated rate law gives normal first-order decay for the reactant,  $B_{\sigma}$ :

$$[B]_{\sigma} = [B]_{o\sigma} e^{-k_{\text{obs}} t} \quad (k_d \ll k_a) \quad 5.4.12$$

and first-order growth for the product,  $AB_{\sigma}$ . Using this last equation and the mole balance, Eq. 5.4.4, gives the integrated time course for the surface-bound complex:

$$[AB]_{\sigma} = [B]_{o\sigma} (1 - e^{-k_{\text{obs}} t}) \quad (k_d \ll k_a) \quad 5.4.13$$

The observed association phase rate constant,  $k_{\text{obs}}$ , is determined by fitting the kinetic time course for each initial A concentration to Eq. 5.4.13. Using Eq. 5.4.10, a plot of  $k_{\text{obs}}$  versus  $[A]_o$  then gives a straight line with slope  $k_a$  and intercept  $k_d$ , Figure 5.4.3.

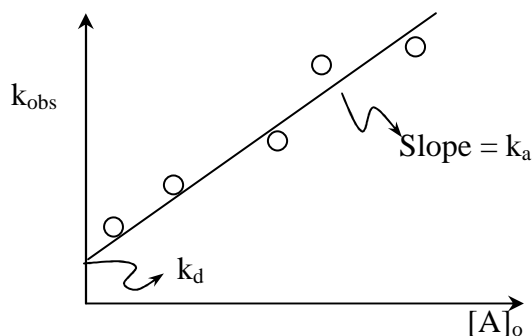


Figure 5.4.3: Extracting the association and dissociation rate constants from a series of experiments with varying analyte concentration.

Notice that these equations assume a constant concentration of flowing analyte; this system is another example of a constant flow chemical reactor. Eq. 5.4.13 also assumes a large association equilibrium constant. In other words, we assume the adsorption reaction runs essentially to completion. If the association constant is not large, the corresponding approach to that given by Eq. 3.4.23-24 must be used for solving for the association phase integrated rate law.

*Dissociation Phase:* The integrated rate law for the dissociation phase is simpler since only buffer is flowing over the surface and then  $[A] \cong 0$ . Eq. 5.4.2 then reduces to:

$$\frac{d[AB]_{\sigma}}{dt} = -k_d [AB]_{\sigma} \quad 5.4.14$$

which is once again a simple first-order process. The concentration of the surface-bound complex then decreases exponentially with rate constant  $k_d$ :

$$[AB] = [AB]_{o\sigma} e^{-k_d t} \quad 5.4.15$$

where  $[AB]_{o\sigma}$  is the surface concentration at the end of the association phase. For a series of experiments with increasing  $[A]_o$  the observed association rate constant will increase, but the observed dissociation rate constant should remain the same for each run. The association phase  $k_{obs}$  is often called the “on rate constant,”  $k_{on}$ , and  $k_d$  the “off rate constant,”  $k_{off}$ .<sup>9,10</sup>

Surface adsorption also plays a very important role in surface catalysis. Surface catalysis can be performed by membrane-bound enzymes, environmental particles, and industrial catalysts.

## 5.5 Solid Surfaces Can Catalyze Chemical Reactions

**Heterogeneous** reactions involve reactants and/or products that are in different phases. One important example is the catalysis of gas phase reactions on solid surfaces. Heterogeneous catalysis is important in atmospheric environmental chemistry. One example is the destruction of ozone in the stratosphere, which involves reactions on frozen nitric acid hydrates.<sup>12</sup> Tropospheric processes can take place on ice crystals in cirrus clouds and on soot or ammonium sulfate particles.<sup>13</sup> Many industrial processes are dependent on heterogeneous catalysis, including the production of ammonia, nitric acid, sulfuric acid, and methanol. Fischer-Tropsch processes are a possible source of transportation fuels from biomass that may be helpful in decreasing our dependence on petroleum. The reactions that are mediated on solid surfaces are easily addressed using the adsorption kinetics principles that we have been developing.

Surface catalysis can be divided into three steps: (1) adsorption on the catalytic surface, (2) the chemical reaction, and (3) desorption of the products. Each step can be the bottleneck in the overall process. Reactants and products can be either weakly or strongly adsorbed. As our first example, consider a first-order reaction that is catalyzed by a surface that starts with the reversible adsorption of the reactant followed by the reaction on the surface. Assume the product is very weakly adsorbed. Adding the surface reaction to Eq. 5.3.4 gives:



where  $k_{\sigma}$  is the rate of the reaction to form products on the surface. Assume that the surface adsorption/desorption steps are in equilibrium, so that we can treat the overall process by a rapid pre-equilibrium mechanism; this is, assume  $k_a, k_d \gg k_{\sigma}$ . The rate law for the reaction, in terms of the extent of the reaction in moles, is given by:

$$\frac{1}{\sigma} \frac{d\xi}{dt} = k_{\sigma} [A]_{\sigma} \quad 5.5.2$$

We can then use Eq. 5.3.3 to relate the rate to the fractional surface coverage:

$$\frac{1}{\sigma} \frac{d\xi}{dt} = k_{\sigma} [B]_{o\sigma} \theta_A \quad 5.5.3$$

Since only molecules in contact with the surface have access to catalytic sites, we only need to consider adsorption onto a single monolayer and we can use Eq. 5.3.11 to model the surface coverage using the Langmuir adsorption isotherm:

$$\frac{1}{\sigma} \frac{d\xi}{dt} = k_{\sigma} [B]_{o\sigma} \frac{b_A P_A}{1 + b_A P_A} \quad (\text{monolayer}) \quad 5.5.4$$

where  $b_A$  is the Langmuir coefficient for the adsorption of the reactant on the surface. Instead of the extent of the reaction on the surface, we often want to relate the reaction rate to the partial pressure of the reactant in the gas phase,  $P_A$ . If we assume that the total moles of reactant on the surface are small compared to the moles of reactant in the gas phase then:

$$\frac{RT}{V} \frac{d\xi}{dt} = -\frac{dP_A}{dt} = \frac{dP_P}{dt} \quad 5.5.5$$

where  $V$  is the volume of the vessel for gases or the volume of solution. Substituting this last equation into the rate law, Eq. 5.5.4 gives the final result we are looking for:

$$-\frac{dP_A}{dt} = [k_\sigma(RT) \sigma/V [B]_{\text{os}}] \frac{b_A P_A}{1 + b_A P_A} \quad (\text{monolayer}) \quad 5.5.6$$

Notice that the rate of the reaction is directly proportional to the active surface area of the catalyst. Also notice the  $\sigma/V$  term is analogous to the  $A/V$  term in calculating photochemical rates, Eqs. 5.1.6 and 5.1.10. The constants in brackets are combined to give an effective rate constant,  $k$ :

$$-\frac{dP_A}{dt} = k \frac{b_A P_A}{1 + b_A P_A} \quad (\text{monolayer}) \quad 5.5.7$$

with  $k = [k_\sigma(RT) \sigma/V [B]_{\text{os}}]$ . Eq. 5.5.7 is empirically found to apply to many reactions under a wide variety of circumstances. Often reactions are even simpler; if the reactant is weakly adsorbed on the surface we can use Eq. 5.3.12 as an estimate of the fractional coverage to give:

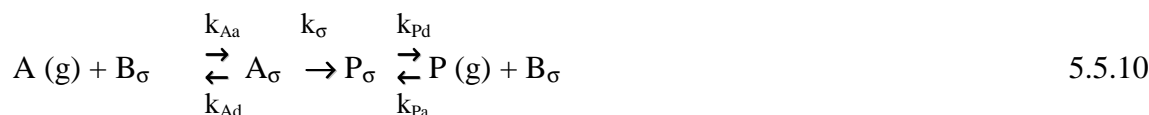
$$-\frac{dP_A}{dt} = k b_A P_A \quad (\text{monolayer, weakly adsorbed}) \quad 5.5.8$$

Such a reaction is said to be a first-order heterogeneous reaction, and an observed rate constant,  $k_{\text{obs}}$ , is defined as  $k_{\text{obs}} \equiv k b_A$ . In other words, the reaction acts like any other first-order reaction except that the reaction is accelerated by interaction with the catalyst surface. If  $A$  is strongly adsorbed, then we can use Eq. 5.3.13 as an estimate of the fractional coverage and then the rate law is zeroth-order in  $A$ :

$$-\frac{dP_A}{dt} = k \quad (\text{monolayer, strongly adsorbed}) \quad 5.5.9$$

The decomposition of  $\text{NH}_3$  on tungsten and the dissociation of  $\text{HI}$  on gold are zeroth-order (see Example 3.2.4). In summary, assuming the surface reaction is the rate determining step, if the reactant is weakly or moderately adsorbed by the surface, then the reaction rate is proportional to the reactant pressure or concentration. If the reactant is strongly adsorbed on the surface, the reaction rate is independent of the reactant pressure or concentration. The preceding mechanisms assume that the product is not strongly adsorbed on the surface. However, if the product is strongly adsorbed, the slow rate for  $P$  leaving the surface will block adsorption sites for the incoming reactant and lead to inhibition.

*Product Inhibition:* Surface catalysis can show strong inhibition if the products of the reaction are strongly adsorbed on the surface. In other words, considering the three steps in surface catalysis, (1) adsorption on the catalyst, (2) the chemical reaction, and (3) desorption of the products, the desorption step may become the rate limiting step. Consider the mechanism:



with  $k_{\sigma}$  the smallest rate constant. As a first approximation, we usually wouldn't consider steps that come after the rate determining step. However, in this case, strong adsorption of P on the surface blocks free sites for adsorption of the reactant. A useful approximation is to start with Eq. 5.3.5 and add the surface reaction:

$$\frac{d[A]_{\sigma}}{dt} = k_{Aa} [B]_{\sigma} P_A - k_{Ad} [A]_{\sigma} - k_{\sigma} [A]_{\sigma} \quad 5.5.11$$

where  $k_{Aa}$  and  $k_{Ad}$  are the adsorption and desorption rate constants for the reactant, respectively. Assuming a steady state for the surface-bound A as the reactive intermediate gives:

$$k_{Aa} [B]_{\sigma} P_A - k_{Ad} [A]_{\sigma} - k_{\sigma} [A]_{\sigma} = 0 \quad \text{or} \quad [A]_{\sigma} = \frac{k_{Aa} [B]_{\sigma} P_A}{k_{Ad} + k_{\sigma}} \quad (\text{steady state}) \quad 5.5.12$$

The Langmuir coefficient for A is defined as  $b_A = k_{Aa}/k_{Ad}$ . If the surface reaction is the slow step,  $k_{\sigma}$  in the denominator can be neglected:

$$[A]_{\sigma} = b_A [B]_{\sigma} P_A \quad (\text{steady state}) \quad 5.5.13$$

To find  $[B]_{\sigma}$  assume that A is weakly adsorbed on the surface. Then, the concentration of free sites will be dominated by the presence of adsorbed product:

$$[B]_{\sigma} = [B]_{o\sigma} (1 - \theta_P) \quad (\text{weak A and strong P adsorption}) \quad 5.5.14$$

where  $\theta_P$  is the fractional coverage of the surface assuming only P is adsorbed. If P is strongly adsorbed, we can estimate the fraction of free sites using Eq. 5.3.15:

$$[B]_{\sigma} = \frac{[B]_{o\sigma}}{b_P P_P} \quad (\text{weak A and strong P adsorption}) \quad 5.5.15$$

where  $P_P$  is the partial pressure of the products in the reaction vessel, and the Langmuir coefficient for adsorption of the product is  $b_P = k_{Pd}/k_{Pa}$ . Substituting Eq. 5.5.13 and 5.5.15 into the rate law, Eq. 5.5.2, gives:

$$\frac{1}{\sigma} \frac{d\xi}{dt} = k_{\sigma} b_A \frac{[B]_{o\sigma} P_A}{b_P P_P} \quad (\text{rapid pre- and post-equilibrium}) \quad 5.5.16$$

Using Eq. 5.5.5 and defining the observed rate constant using all of the constants in this last equation with  $k_{obs} \equiv k_{\sigma} b_A \sigma/V [B]_{o\sigma}/b_P$  gives:

$$-\frac{dP_A}{dt} = k_{obs} \frac{P_A}{P_P} \quad (\text{weak A and strong P adsorption}) \quad 5.5.17$$

The appearance of the partial pressure of the products in the denominator shows that the reaction is inhibited as P builds up on the surface. Near equilibrium with significant concentrations of product, Eq. 5.5.17 appears as a pseudo-first-order process. For such a reaction to be useful, an active mechanism to remove the product gas from the reaction vessel is necessary. Note that the

observed rate constant,  $k_{\text{obs}}$ , is directly proportional to the catalyst surface area, as we would intuitively expect.

The important points to remember from our consideration of heterogeneous catalysis is (1) that the definition of surface concentration allows us to use the machinery of chemical kinetics that we developed for homogenous reactions, (2) the surface is often the limiting reagent, (3) the rate is directly proportional to the surface area. Much of the development of catalytic systems is in maximizing the active catalytic surface area. The use of nanoparticle-based catalysts is an important approach to maximizing surface area and catalytic activity.<sup>14</sup>

---

**Example 5.5.1:**

The catalytic hydrogenation of cyclopropane on nickel has been studied as a function of the initial pressures of the reactants at 122°C.<sup>15</sup> Determine the order of the reaction with respect to cyclopropane and hydrogen from the data in the table, below. Discuss the state of adsorption of each reactant on the surface.

$P_{\text{cyclopropane}}$ (torr)	$P_{\text{H}_2}$ (torr)	Initial Rate (torr min <sup>-1</sup> )
100	200	1.00
200	200	1.95
400	200	3.80
100	100	1.10
100	400	1.25

*Answer:* Following the initial rate for changes in the pressure of cyclopropane, while holding  $P_{\text{H}_2}$  constant, shows approximate first-order dependence. The initial rate doubled on doubling  $P_{\text{cyclopropane}}$  and the initial rate increased by a factor of about four when  $P_{\text{cyclopropane}}$  was increased by a factor of four. Following the data for  $P_{\text{cyclopropane}} = 100$  shows the initial rate to be roughly constant with increasing  $P_{\text{H}_2}$ . The constant rate shows a zeroth-order dependence on  $\text{H}_2$ . Comparing these results to Eqs. 5.5.8 and 5.5.9 suggests that cyclopropane is weakly adsorbed, while  $\text{H}_2$  is strongly adsorbed.

---

## 5.6 Summary – Looking Ahead

Photochemistry and surface chemistry play an important role in many processes, including photosynthesis, biogeochemical processes in the atmosphere, and industrial processes. Photochemistry and surface chemistry will also make increasingly important contributions to solving global issues in energy production and pollution abatement. These practical problems also involve spatial variation in chemical concentrations. In fact, concentration gradients are a general means for converting one form of chemical energy into another. The coupling of chemical reactions with spatial variation is discussed in the next chapter. Practical problems are often quite complex. The chemical processes that determine the interrelationships are modeled by networks of differential equations. These networks are often illustrated by box models, as in Figure 5.1.1. The next chapter also introduces box models and the analysis of complex networks of chemical reactions and spatial processes.

## 5.7 Addendum: *MatLab* Files for the Chapman Ozone Mechanism

The differential equations are defined, with all the constants, in a function file, “chapman.m”:<sup>16</sup>

```
function dX = chapman(t,X);
% Constants for 40 km:
j1=5.7e-10;
k2=9.1e-34;
j3=1.9e-3;
k4=2.2e-15;
M=8.1e16;
%Differential equations
dX = zeros(3,1);
dX(1) = 2*j1*X(2)-k2*X(1)*X(2)*M+j3*X(3)-k4*X(1)*X(3);
dX(2) = -j1*X(2)-k2*X(1)*X(2)*M+j3*X(3)+2*k4*X(1)*X(3);
dX(3) = k2*X(1)*X(2)*M-j3*X(3)-k4*X(1)*X(3);
```

The main routine, “ozone40km.m,” sets the initial conditions, time range, solves the equations, and specifies plots for the three concentrations:

```
clear
% Set the initial values
Xo = [0 1.7e16 0];
% Set the total integration time in seconds
maxTime = 3.5e5;
trange = [0 maxTime];

% solve the differential equations
[T,X] = ode15s(@chapman,trange,Xo);

% Plot data
figure(1)
plot(T,X(:,1))
title('[O] at 40 km')
xlabel('Time (sec)')
ylabel('[O] (molecules cm-3)')

%
figure(2)
plot(T,X(:,2))
title('[O2] at 40 km')
xlabel('Time (sec)')
ylabel('[O2] (molecules cm-3)')

%
figure(3)
plot(T,X(:,3))
title('[O3] at 40 km')
xlabel('Time (sec)')
ylabel('[O3] (molecules cm-3)')
```

The solver “ode15s” is a moderate accuracy stiff differential equations solver. A more accurate, but much slower solver is the 4<sup>th</sup> order Runge-Kutta solver, “ode45”, which you can try for a timing comparison. The “Kinetic Mechanism Simulation” applet also uses the 4<sup>th</sup> order Runge-Kutta algorithm, but is not as time efficient. These *MatLab* routines can be made significantly more flexible. However, our goal is to show how easily moderately complicated sets of simultaneous differential equations can be solved using readily available simulation software.



## Chapter Summary

### *Photochemistry:*

1. Light must be absorbed by a molecule to initiate a photochemical process.
2. The Stark-Einstein Law of photochemical equivalence states that each absorbed photon results in one primary photochemical process.
3. The quantum yield for fluorescence is  $\Phi_f = J_f/J_a$ , with the emitted light flux,  $J_f$ , and the absorbed light flux,  $J_a$ . The quantum yield for the production of a secondary photoproduct, B, is given by:  $\Phi_B = (d[B]/dt)/J_a$ .

4. The incident flux in  $\text{mol L}^{-1} \text{s}^{-1}$  is:  $J_o = \frac{J_o}{N_A h\nu} \left( \frac{\mathcal{A}}{V} \right)$

with  $J_o$  the incident flux in  $\text{watts m}^{-2} \text{s}^{-1}$ , the incident beam cross sectional area  $\mathcal{A}$  in  $\text{m}^2$ , and the volume of the solution  $V$  in L.

5. The absorbed flux is  $J_a = J_o (1 - e^{-2.303 \epsilon [A] \ell})$ , given the concentration  $[A]$ , the molar absorption coefficient of the solution,  $\epsilon$ , and the path length  $\ell$ .
6. The rate law for the formation of secondary photoproduct is:

$$\frac{d[B]}{dt} = \Phi_B J_a = \Phi_B J_o (1 - e^{-2.303 \epsilon [A] \ell})$$

with  $\Phi_B$  the quantum yield for the production of B. For optically thick systems,  $J_a = J_o$ , giving the zeroth-order rate law:  $(d[B]/dt) = \Phi_B J_o$ . For optically thin systems the rate law is first order:  $(d[B]/dt) = j_B [A]$  with  $j_B = 2.303 J_o \Phi_B \epsilon \ell$ .

7. During photolysis, the formation of the secondary photoproduct is in competition with all processes that deactivate the primary photoproduct. Assuming a first-order or pseudo-first order process with rapid deactivation,  $A^* \rightarrow B$ , the quantum yield is:  $\Phi_B = k_R / (k_f + k_{ISC} + k_{nr} + k_R)$ , with the rate constants for the reaction from the excited state  $k_R$ , fluorescence  $k_f$ , intersystem crossing  $k_{ISC}$ , and non-radiative collisional processes  $k_{nr}$ .
8. Fluorescence is in competition with all processes that deactivate the primary photoproduct. The fluorescence quantum yield is  $\Phi_f = J_f/J_a = k_f / (k_f + k_{ISC} + k_{nr} + k_R)$ .
9. The Stern-Volmer mechanism for fluorescence quenching, with the quantum yield without quencher present,  $\Phi_o$ , and the quantum yield with quencher present,  $\Phi_f$ , gives:

$$\Phi_o/\Phi_f = I_o/I = \frac{k_f + k_{ISC} + k_{nr} + k_q[Q]}{k_f + k_{ISC} + k_{nr}} = 1 + \frac{k_q[Q]}{k_f + k_{ISC} + k_{nr}}$$

10. After irradiation, first-order competitive processes deactivate the excited state and the lifetime of the excited state is  $1/\tau = k_f + k_{ISC} + k_{nr} + k_R = 1/\tau_f + 1/\tau_{ISC} + 1/\tau_{nr} + 1/\tau_R$ .

### *Surface Chemistry:*

11. Physical adsorption is the rapid and reversible interaction of a substance with a surface through non-covalent forces, such as hydrogen-bonding, dipolar forces, and dispersion forces. Chemical adsorption involves the formation of covalent bonds to surface atoms or strong ionic interactions.
12. Absorption occurs when molecules fill voids in a porous surface or form multiple layers beyond the first adsorbed layer.

13. The surface concentration of species A on the surface is defined as  $[A]_{\sigma} \equiv n_{A\sigma}/\sigma$ , where  $n_{A\sigma}$  is the number of moles of A on the surface and  $\sigma$  is the surface area. The surface concentration of the free binding sites on the surface,  $[B]_{\sigma} \equiv n_{B\sigma}/\sigma$  where  $n_{B\sigma}$  is the number of moles of free binding sites on the surface, may be the limiting reagent in a surface interaction.
14. The fractional coverage of A on a surface,  $\theta_A$ , is:  $\theta_A = [A]_{\sigma}/[A]_{\max\sigma} = n_{A\sigma}/n_{A\max\sigma}$
15. The mechanism for monolayer surface adsorption with equivalent sites can be approximated by  $A(g) + B_{\sigma} \rightleftharpoons A_{\sigma}$ . Given  $k_a$ , the rate constant for adsorption, and  $k_d$  the rate constant for desorption, the Langmuir coefficient for the surface interaction is  $b = k_a/k_d$ .
16. The Langmuir adsorption isotherm gives the fractional coverage at equilibrium:  $\theta_A = b P_A/(1 + b P_A)$ . For low partial pressures or weak binding, the Langmuir isotherm reduces to:  $\theta_A = b P_A$ . For large partial pressures or for very strong adsorption the surface coverage reaches a maximum at 100%,  $\theta_A \approx 1$ .
17. The fraction of the surface area that is free is:  $1 - \theta_A = 1/(1 + b P_A)$ . For high partial pressures of A or strong binding the free fraction reduces to:  $1 - \theta_A \approx 1/(b P_A)$ .
18. In a dynamic sensor experiment, the rate of surface adsorption for a high affinity analyte flowing over the surface is  $-(d[B]_{\sigma}/dt) = k_{\text{obs}} [B]_{\sigma}$ , where  $k_{\text{obs}} = (k_a [A]_o + k_d)$ ,  $[B]_{\sigma}$  is the concentration of binding sites on the surface, and  $[A]_o$  is the analyte solution concentration.
19. The rate of surface catalysis for monolayer adsorption is given by:

$$-\frac{dP_A}{dt} = k \frac{b_A P_A}{1 + b_A P_A} \quad \text{with} \quad k = [k_{\sigma} \sigma/V [B]_{o\sigma}]$$

where  $b_A$  is the Langmuir coefficient for the reactant on the surface,  $k_{\sigma}$  is the rate of the reaction on the surface,  $\sigma$  is the surface area,  $V$  is the volume of the vessel for gases or the volume of the solution, and  $[B]_{o\sigma}$  is the maximum concentration of binding sites on the surface. If the reactant is weakly adsorbed on the surface the rate law is first order,  $-dP_A/dt = k b P_A$ . If the reactant is strongly adsorbed the rate law is zeroth order,  $-dP_A/dt = k$ .

20. For surface catalysis with product inhibition, the product remains on the surface blocking adsorption sites for the reactant:

$$-\frac{dP_A}{dt} = k_{\text{obs}} \frac{P_A}{P_P} \quad \text{with} \quad k_{\text{obs}} \equiv k_{\sigma} b_A \sigma/V [B]_{o\sigma}/b_P$$

where  $b_P$  is the Langmuir constant for the interaction of the product with the surface. Near equilibrium with significant concentrations of product the rate law is pseudo-first-order.

## Literature Cited

1. A. Leifer, *The Kinetics of Environmental Aquatic Photochemistry*, American Chemical Society, Washington, DC, 1988. pp. 143-5.
2. A. Kleidon, K. Fraedrich, "Biotic Entropy Production and Global Atmosphere-Biosphere Interactions," in A. Kleidon, R. D. Lorenz (Eds.), *Non-equilibrium Thermodynamics and the Production of Entropy: Life, Earth, and Beyond*, Springer Verlag, Heidelberg, Germany, 2004. Ch. 14.
3. D. Juretić, P. Županović, "Photosynthetic models with maximum entropy production in irreversible charge transfer steps," *Computational Biol. and Chem.*, **2003**, *27*, 541-553.

4. J. S. Winn, *Physical Chemistry*, Harper Collins, 1995. p. 1046.
5. M. Z. El-Din, K. Elsayed, S. M. Al-Sherbini, M. A. Harith, "Photostability of Uranine via Crossed-Beam Thermal Lens Technique," *Laser Chemistry*, **2007**, Article ID 36024, 1-5.
6. E. Harvey, R. Sweeney, "Modeling Stratospheric Ozone Kinetics, Part I The Chapman Cycle," *J. Chem. Ed.*, **1999**, *76*, 1309.
7. W. B. DeMore, C. J. Howard, S. P. Sander, A. R. Ravishankara, D. M. Golden, C. E. Kolb, R. F. Hampson, M. J. Molina, M. J. Kurylo, *Chemical Kinetics and Photochemical Data for Use in Stratospheric Modeling, Evaluation Number 12*, Jet Propulsion Laboratory: Pasadena, 1997 (JPL Pub. 97-4, <http://remus.jpl.nasa.gov/jpl97/>.)
8. W. Stumm, J. J. Morgan, *Aquatic Chemistry: Chemical Equilibria and Rates in Natural Waters*, 3rd Ed., Wiley, New York, NY, 1996. pp. 521-8.
9. D. G. Myszka, "Kinetic, equilibrium, and thermodynamic analysis of macromolecular interactions with BIACORE," *Methods in Enzymology*, **2000**, *323*, 325-40.
10. D. G. Myszka, R. L. Rich, "Implementing surface plasmon resonance biosensors in drug discovery," *Pharmaceutical Science & Technology Today*, **2000**, *3(9)*, 310-317.
11. P. Schuck, "Reliable determination of binding affinity and kinetics using plasmon surface resonance biosensors," *Curr. Opin. Biotechnol.*, **1997**, *8(4)*, 498.
12. M. J. Molina, L. T. Molina, C. E. Kolb, "Gas-Phase and Heterogeneous Chemical Kinetics of the Troposphere and the Stratosphere," *Annu. Rev. Chem.*, **1996**, *47*, 327-67.
13. A. R. Ravishankara, "Heterogeneous and Multiphase Chemistry in the Troposphere," *Science*, **1997**, *276*, 1058-1065.
14. B. F.G. Johnson, "Nanoparticles in catalysis," *Topics in Catalysis*, **2003**, *24(1-4)*, 147-159.
15. G. C. Bond and J. Sheridan, "Studies in heterogeneous catalysis. Part 4.—The hydrogenation of cyclopropane," *Trans. Faraday Soc.*, **1952**, *48*, 713 – 715.
16. F. Akhtar, "The Chapman Reactions: A model of the Production and Destruction of Stratospheric Ozone," School of Earth and Atmospheric Sciences, Georgia Institute of Technology: <http://www.prism.gatech.edu/~gte618p/chapman.html>.

## Further Reading

### *Photochemistry*

J. G. Calvert, J. N. Pitts Jr., *Photochemistry*, Wiley, New York, NY, 1966.

C.E. Wayne, R.P. Wayne, *Photochemistry, Oxford Chemistry Primers 39*, Oxford, Oxford, UK, 1996.

A. Leifer, *The Kinetics of Environmental Aquatic Photochemistry*, American Chemical Society, Washington, DC, 1988.

### *Ozone Depletion*

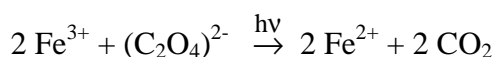
H. Johnston, "Catalytic Reduction of Stratospheric Ozone by Nitrogen Oxides," UCRL-20568, OSTI ID: 4721037, Lawrence Berkeley National Laboratory, Berkeley, CA., 1971.

### *Heterogeneous Processes and Oceanography*

W. Stumm, J. J. Morgan, *Aquatic Chemistry: Chemical Equilibria and Rates in Natural Waters*, 3<sup>rd</sup> Ed., Wiley-InterScience, New York, NY, 1996.

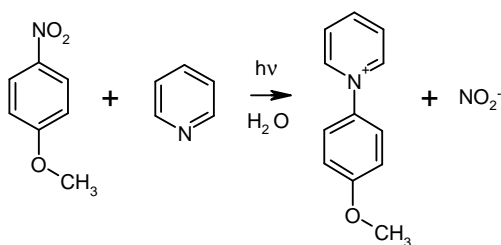
### Problems: Photochemistry and Surface Chemistry

1. Show that the units are correct for Eq. 5.1.15 with  $\epsilon$  in  $\text{M}^{-1} \text{cm}^{-1}$ ,  $\mathcal{A}$  in  $\text{m}^2$ , and  $V$  in liters in Eq. 5.1.6.
2. Show that the photochemical rate constant for an optically thin solution is independent of path length for a cell with a uniform cross section. For example, a cell with uniform cross section includes cylindrical cells and rectangular cells where the volume is given by the area of the solution exposed on the face of the cell,  $a$ , multiplied by the path length,  $V = a\ell$ . Determine any unit conversion factors in the final result.
3. A chemical actinometer is a solution with known quantum yield that can be used to find the incident intensity in photochemical experiments. The ferrioxalate actinometer uses the reaction:



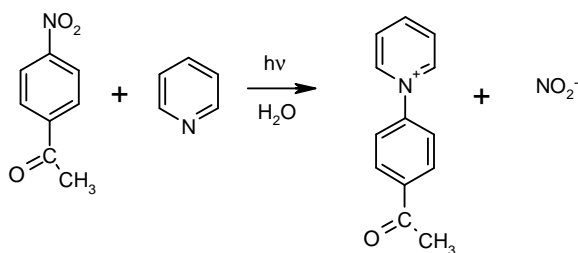
A ferrioxalate concentration of 0.15 M is normally used for actinometry, which is optically thick. A common light source for photochemical reactions is the 366 nm emission line of a mercury lamp. The quantum yield for the ferrioxalate reaction at 366 nm is 1.18.<sup>1</sup> The progress of the reaction is monitored using the visible absorption of the *ortho*-phenanthroline complex of  $\text{Fe}^{2+}$  at 522 nm. The molar absorption coefficient of the  $\text{Fe}^{2+}$  complex at 522 nm is  $8650 \text{ M}^{-1} \text{cm}^{-1}$ . The *ortho*-phenanthroline complex for  $\text{Fe}^{3+}$  is very weak and transparent at 522 nm. The following experiment was used to determine the incident intensity for a photoreactor. A solution of 0.15 M ferrioxalate was irradiated for 10.0 min. A 1.00 mL aliquot was withdrawn and diluted with water to a total volume of 100.0 mL in a volumetric flask. The absorbance of this solution in a 1.00 cm pathlength cuvette at 522 nm was 0.410. Calculate the incident flux in  $\text{mol L}^{-1} \text{s}^{-1}$ .

4. A high power mercury lamp produces  $219.0 \text{ W m}^{-2}$  at 366 nm at the surface of a photochemical reaction cell (see Problem 3). Assume the cross-section of the incident beam is  $1.00 \text{ cm}^2$  and the solution volume is 10.0 mL. Calculate the incident flux in  $\text{mol L}^{-1} \text{s}^{-1}$ .
5. When *p*-nitroanisole and pyridine are photolyzed in aqueous solution the reaction is:



The quantum yield for a solution containing  $1.00 \times 10^{-5} \text{ M}$  *p*-nitroanisole and 0.0100 M pyridine in 1% acetonitrile is  $4.65 \times 10^{-3}$  at 366 nm.<sup>2</sup> The molar absorption coefficient at 366 nm of *p*-nitroanisole is  $1990 \text{ M}^{-1} \text{cm}^{-1}$ . Calculate the photochemical rate constant and write the rate law for an optically thin solution assuming the incident flux is  $6.70 \times 10^{-6} \text{ mol L}^{-1} \text{s}^{-1}$  for a 10.00 cm path length reaction cell.

6. A solution with a known photochemical quantum yield can be used to calculate the incident light flux during a photolytic reaction. Such solutions are called chemical actinometers (see Problems 3 and 5). Consider the reaction of *p*-nitroacetophenone and pyridine:



A chemical actinometer and a solution of *p*-nitroacetophenone and pyridine were simultaneously photolyzed at 366 nm in reaction cells with identical geometry. The path length of the reaction cell is 1.00 cm. The quantum yield for the actinometer is  $4.65 \times 10^{-3}$  with a molar absorption coefficient  $1990 \text{ M}^{-1} \text{ cm}^{-1}$ . The photochemical rate constant for the actinometer is determined to be  $1.43 \times 10^{-3} \text{ s}^{-1}$ . The molar absorption coefficient of *p*-nitroacetophenone is  $160. \text{ M}^{-1} \text{ cm}^{-1}$ .<sup>2</sup> The photochemical rate constant for  $1.00 \times 10^{-5} \text{ M}$  *p*-nitroacetophenone and  $0.100 \text{ M}$  pyridine is  $4.18 \times 10^{-5} \text{ s}^{-1}$ . Calculate the quantum yield for the *p*-nitroacetophenone and pyridine reaction at 366 nm.

7. Consider the following reversible first-step mechanism for a first-order photochemical reaction:



where  $k_D$  is the combined rate constant for all the non-photochemical deactivation processes, with  $k_D = k_f + k_{\text{ISC}} + k_{\text{nr}}$ . Derive Eq. 5.1.24 directly from this mechanism. [Hint: Express the rate law in the form of Eq. 5.1.17 and then use Eq. 5.1.19]

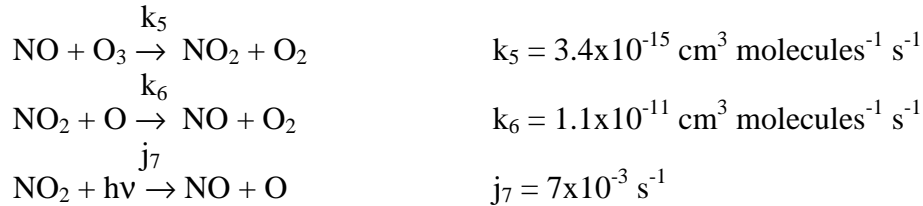
8. Anthracene fluorescence is quenched by halogenated compounds like  $\text{CCl}_4$ . A Stern-Volmer quenching study was completed giving the fluorescence intensities, as a function of  $\text{CCl}_4$  concentration, in the following table.<sup>3</sup> The intensities are in arbitrary units. The fluorescence lifetime in the absence of  $\text{CCl}_4$  is 5.03 ns. Calculate the quenching rate constant.

$[\text{CCl}_4] \text{ (M)}$	0	0.02	0.04	0.08	0.12
Intensity	2437	1860	1490	1110	893

9. Run a numerical simulation for the Chapman mechanism for the rate constants and concentrations appropriate at an altitude of 25 km. A table of appropriate constants is given below.<sup>4,5</sup> Determine the steady-state concentration of ozone using Eq. 5.2.11 and by numerical simulation.

Altitude km	$j_1$ $\text{s}^{-1}$	$k_2$ $\text{cm}^6 \text{ molecule}^{-2} \text{ s}^{-1}$	$j_3$ $\text{s}^{-1}$	$k_4$ $\text{cm}^3 \text{ molecule}^{-1} \text{ s}^{-1}$	$[\text{M}]$ $\text{molecule cm}^{-3}$	$[\text{O}_2]$ $\text{molecule cm}^{-3}$
25	$3.0 \times 10^{-12}$	$1.2 \times 10^{-33}$	$5.5 \times 10^{-4}$	$6.9 \times 10^{-16}$	$9 \times 10^{17}$	$1.8 \times 10^{17}$
40	$5.7 \times 10^{-10}$	$9.1 \times 10^{-34}$	$1.9 \times 10^{-3}$	$2.2 \times 10^{-15}$	$8.1 \times 10^{16}$	$1.7 \times 10^{16}$

10. Nitrogen oxides catalyze the destruction of ozone and must be taken into account in accurate stratospheric models. The reactions and the rate constants appropriate for 25 km are:



The values for the rate constants  $j_1$ - $k_4$  and  $[M]$  at 25 km are given in Problem 9. Guesses for the starting concentrations for NO and  $\text{NO}_2$  that you can use are:

$$[\text{NO}]_0 = 8.0 \times 10^8 \text{ molecules cm}^3 \quad \text{and} \quad [\text{NO}_2] = 1.0 \times 10^9 \text{ molecules cm}^3$$

Add these three reactions to the numerical simulation outlined in Addendum 5.7 to find the change of the ozone concentration with and without catalysis. You can use *MatLab* or *MathCad*, or any numerical routines that employ stiff methods.

11. Problem 10 lists the three reactions that supplement the Chapman mechanism to account for the catalytic destruction of ozone caused by NO and  $\text{NO}_2$ . (a) At steady state, show that the rate law for odd oxygen species can be expressed as:

$$\frac{d([\text{O}_3] + [\text{O}])}{dt} = 2 j_1 [\text{O}_2] - 2 k_4 [\text{O}_3][\text{O}] \left( 1 + \frac{k_6 [\text{NO}_2]}{k_4 [\text{O}_3]} \right)$$

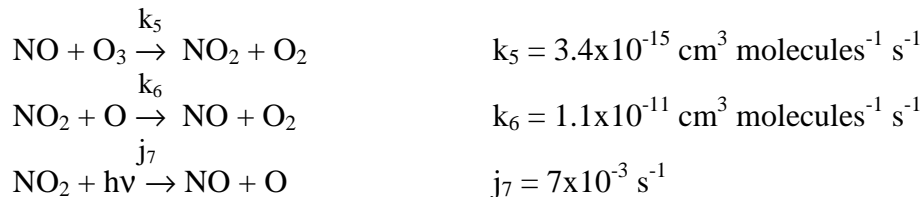
The term in parentheses is called the enhancement factor,  $\rho$ :

$$\rho = \left( 1 + \frac{k_6 [\text{NO}_2]}{k_4 [\text{O}_3]} \right)$$

which determines the extent of the catalysis of the destruction of ozone by NO and  $\text{NO}_2$ . Use the rate constants given in Problems 9 and 10 along with the following rough estimates for the steady-state concentrations to estimate the enhancement factor at 25 km. These concentrations are from the results of Problem 10 at 25 km:

$$[\text{O}_3] = 8.74 \times 10^{12} \text{ molecules cm}^{-3} \quad [\text{NO}_2] = 1.45 \times 10^9 \text{ molecules cm}^{-3}$$

12. Nitrogen oxides catalyze the destruction of ozone and must be taken into account in accurate stratospheric models. The reactions and the rate constants appropriate for 25 km are:



Show that the ratio of the  $\text{NO}_2$  and NO concentrations at steady-state are given by the relationship:

$$\frac{[\text{NO}_2]}{[\text{NO}]} = \frac{k_5 [\text{O}_3]}{k_6 [\text{O}] + j_7}$$

Calculate the steady-state ratio assuming that the O atom concentration is small enough that  $k_6[\text{O}] \ll j_7$ . Assume  $[\text{O}_3] = 8.74 \times 10^{12}$  molecules  $\text{cm}^{-3}$  (as in Problem 11).

13. The combustion of carbon sources, such as coal or charcoal, in limited amounts of oxygen produces carbon monoxide. Carbon monoxide is a commonly used reducing agent, especially in metallurgy. The reaction of carbon with high temperature steam produces carbon monoxide and hydrogen gas. Carbon monoxide and hydrogen are the feed stocks for industrial processes like the Fischer-Tropsch process, which can be used to produce transportation fuels from coal or biomass. Carbon monoxide readily adsorbs onto charcoal surfaces. The equilibrium surface loading of CO on charcoal at 0°C is given in the following table. Determine the Langmuir coefficient for this system.

Pco (bar)	0.0973	0.240	0.412	0.720	1.176
$\Gamma$ (mmol $\text{g}^{-1}$ )	0.113	0.248	0.378	0.573	0.787

14. Antibody-antigen interactions are very strong and very specific. The interaction between a protein, bovine serum albumin, and anti-BSA immunoglobulin G (IgG) was determined using SPR. BSA was attached to a gold surface and the IgG was flowed over the surface at constant concentration. The results for the observed association rate constant are given in the table below. The dissociation rate constants, from nonlinear curve fitting from the time courses, were averaged over each run and found to be  $5.94 \times 10^{-5} \text{ s}^{-1}$ . Find  $k_a$ , the association equilibrium constant,  $K_A$ , and the dissociation equilibrium constant,  $K_D$ . Convert  $K_D$  to picomolar units, pM, which is typical of the conventional choice of units in the medicinal chemistry literature.

[IgG] (nM)	10.0	4.00	1.60	0.640
$k_{\text{obs}}$ ( $\text{s}^{-1}$ )	0.00623	0.002914	0.001578	0.00057

15. SPR is a commonly used technique in immunology. The interaction between a protein, porcine serum albumin, PSA, and anti-PSA immunoglobulin G (IgG) was determined using SPR. The anti-PSA IgG was attached to a gold surface and PSA was flowed over the surface at constant concentration. The results for the observed association rate constant are given in the table below.<sup>6</sup> The dissociation rate constants, from nonlinear curve fitting from the time courses, were averaged over each run and found to be  $1.02 \times 10^{-3} \text{ s}^{-1}$ . Find  $k_a$ , the association equilibrium constant,  $K_A$ , and the dissociation equilibrium constant,  $K_D$ . Convert  $K_D$  to nanomolar units, nM, which is typical of the conventional choice of units in the medicinal chemistry literature.

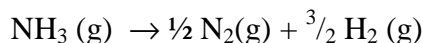
[PSA] (nM)	7.18	21.5	66.4	201.	601.
$k_{\text{obs}}$ ( $\text{s}^{-1}$ )	0.0122	0.00189	0.00189	0.0297	0.0641

16. It is not necessary in dynamic SPR measurements to wait for the surface adsorption to reach equilibrium. However, if the time course for the association does essentially reach equilibrium, the equilibrium values can be fit to the Langmuir adsorption isotherm. Such equilibrium SPR experiments provide an alternative method to determine the equilibrium dissociation constant that is complementary to dynamic measurements. Comparison between equilibrium and dynamic results helps to determine experimental uncertainties. The limiting refractive index values from the time course measurements for the system in Problem 15 are given below.<sup>6</sup> By fitting the results to a Langmuir adsorption isotherm, determine the equilibrium dissociation constant in

nanomolar units. The units typical for SPR instrument output are micro-refractive index units, or  $\mu\text{RIU}$ .

[PSA] (nM)	0	7.18	7.18	19.7	59.2	181.3	538.5
R ( $\mu\text{RIU}$ )	0	23.6	26.5	38	55.6	57.6	58.8

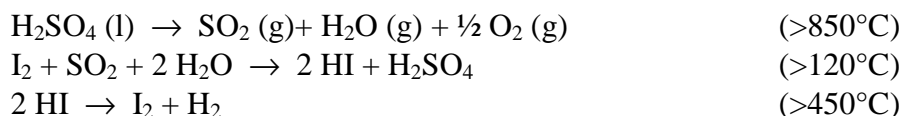
17. The rate of decomposition of  $\text{NH}_3$  was determined as a function of the initial partial pressure of  $\text{H}_2$  and is inhibited by product formation:<sup>7</sup>



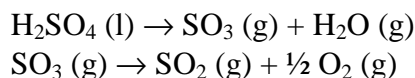
The initial pressure of  $\text{NH}_3$  in each run was 100 mm Hg, and varying amounts of  $\text{H}_2$  gas were added to the reaction vessel at the beginning of the reaction. The catalyst was platinum and the reaction was run at  $1138^\circ\text{C}$ . The results are given below. Show that the dependence on the product,  $\text{H}_2$ , partial pressure is described by Eq. 5.5.17.

$\Delta P_{\text{NH}_3}$ in 120 s	$P_{\text{H}_2}$ initially added
33	50
27	75
16	100
10	150

18. Hydrogen is a clean burning substance that is being suggested as a transportation fuel. However, hydrogen is costly to produce. One proposal is to use solar thermal energy to provide the energy necessary to convert water into hydrogen gas. The Sulfur-Iodine cycle consists of three coupled reactions, which add to give the dissociation of water:



The first step is the most unfavorable thermodynamically and kinetically. The reaction occurs in two steps:

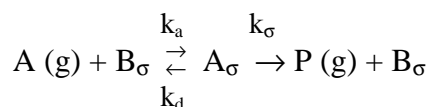


The decomposition of  $\text{SO}_3$  has a negligible rate at  $800^\circ\text{C}$  without a catalyst. Mixed chromium-iron oxide catalysts have been proposed for the gas phase decomposition of  $\text{SO}_3$ .<sup>8</sup> The heterogeneous decomposition of  $\text{SO}_3$  on  $\text{Fe}_{1.6}\text{Cr}_{0.4}\text{O}_3$  in a constant flow reactor has been studied as a function of temperature. The percent yields at several temperatures are given in the table, below. The residence time of the reactant in a constant flow reactor is constant with temperature, so the percent yield is directly proportional to the reaction rate. Verify Arrhenius behavior and determine the activation energy.

T ( $^\circ\text{C}$ )	550	600	650	750	800
$\text{SO}_2$ yield %	1.2	5.5	10.7	52.7	79.3



19. Derive the rate law for a bimolecular heterogeneous reaction with stoichiometry:  $A + C \rightarrow P$ . Assume that reactant C is strongly adsorbed to the catalytic surface and A is weakly adsorbed.
20. Determine the integrated rate law for surface catalysis from an adsorbed monolayer using Eq. 5.5.7.
21. We assumed a pre-equilibrium mechanism to determine the rate for a heterogeneously catalyzed reaction proceeding according to Eq. 5.5.1:



The rate law for the reaction, in terms of the products is then given by:

$$\frac{d[P]}{dt} = k_{\sigma}(RT) (\sigma/V) [A]_{\sigma}$$

To give a better approximation, use the steady-state approximation to determine the rate law. Then show that the more exact rate law reduces to Eq. 5.5.6 using a suitable approximation.

### Literature Cited

1. A. Leifer, *The Kinetics of Environmental Aquatic Photochemistry*, American Chemical Society, Washington, DC, 1988. pp. 149-50.
2. A. Leifer, *The Kinetics of Environmental Aquatic Photochemistry*, American Chemical Society, Washington, DC, 1988. pp. 106-10.
3. W. Legenza, C. J. Morzzacco, "The Rate Constant for Fluorescence Quenching, An undergraduate experiment using the Spectronic 20," *J. Chem. Ed.*, **1977**, *54*, 183-184.
4. F. Akhtar, "The Chapman Reactions: A model of the Production and Destruction of Stratospheric Ozone," School of Earth and Atmospheric Sciences, Georgia Institute of Technology: <http://www.prism.gatech.edu/~gte618p/chapman.html>
5. E. Harvey, R. Sweeney, "Modeling Stratospheric Ozone Kinetics, Part I The Chapman Cycle," *J. Chem. Ed.*, **1999**, *76*, 1309.
6. T. Ryan, Reichert Analytical Instruments, Depew, NY, private communication.
7. C. N. Hinshelwood, R. E. Burk, "Thermal decomposition of ammonia upon various surfaces," *J. Chem. Soc., Transactions*, **1925**, *127*, 1105-17.
8. A. M. Banerjee, M. R. Pai, K. Bhattacharya, A. K. Tripathi, V. S. Kamble, S. R. Bharadwaj, S. K. Kulshreshtha, "Catalytic decomposition of sulfuric acid on mixed Cr/Fe oxide samples and its application in sulfur-iodine cycle for hydrogen production," *International Journal of Hydrogen Energy*, **2008**, *33*(1), 319-326.

*(Left intentionally blank)*